Anonymous Referee #1

The authors have done much to address the comments of the reviewers and the revised ms is much stronger as a result. I think that readers will benefit from seeing the exchange among authors and reveiwers.
Although the ms is clearly written, the ms still needs a close editorial check for good grammar throughout.
e.g. line 99, "needful" should be "needed". L108 "Thank for recent advances . . ." There are many examples of grammatical errors that need to be corrected. I appreciate that English is not their first language, so they need the aid of a good editor or colleague to correct mistakes.
The terminology "tidal pools" should be used instead of 'ponds'.

Edward Laws, has carefully checked and thoroughly edited the manuscript in terms of language (changes are in blue in the trackable version).

Minor comments

e.g. line 99, "needful" should be "needed".

Corrected.

L108 "Thank for recent advances . . ."

Follow Reviewer #3, we changed it to “As a result of”.

The terminology "tidal pools" should be used instead of 'ponds'.

Changed.

Anonymous Referee #3

The authors have satisfactorily responded to my previous comments, though the editing has muddled the explanation of the model somewhat. I have only minor comments at this point.

Thanks for the reviewer's recognition.

line 108: this should be 'Thanks to' not 'Thanks for'. Probably better to substitute "As a result of"

As suggested, we changed it to "As a result of".

The development of the model was laid out more clearly in the previous version. I am not sure the reviewer comments that brought about this change? At the very least, explicit definition of the source of the atmospheric atm% constant term (0.00366) should be given for unfamiliar readers.

Yes, additional part for model development was added according to previous review. We add the reference of Coplen et al. (1992) for the source of the atmospheric atm% constant term (0.00366).

lines 333-334: N/P ratio below 16 doesn't necessarily mean the system is N limited. 0.5 uM [NO3-] concentration suggests it is not.

We would like to provide more background information originally to show readers P is not limiting during entire incubation. To avoid distraction, we deleted this sentence. Such deletion would not influence the logic flow and story.

lines 392-394: This sentence is unclear.

The sentence "In general, the rates of the first time interval can well predict the following up observations, demonstrating a good predictive performance by using the matrix method instant rate." was changed to "The fact that the rates during the first time interval generally predicted rather well the subsequent observations demonstrated a good predictive performance with the matrix method initial rate."

line 535: These are rate constants, not rates.

Corrected.

line 569: This comment about the author's reply to reviews should not be in the final manuscript.

We decided to add this figure into supplementary information (see Fig. S3).

line 589: I would change this to 'may have been overestimated'

Changed as suggested.

line 608-617: Double check this paragraph for correct usage of RPI, as it there are several typos where it says PRI instead.

We changed to RPI.

The verb tense for many of the sub-headings in Section 4 should be changed, e.g. 4.2.4 should say 'Quantifying' not 'Quantify'

Changed as suggested.

Quantification of multiple simultaneously occurring nitrogen flows in the euphotic ocean

Min Nina Xu[1], Yanhua Wu[2], Li Wei Zheng[1], Zhenzhen Zheng[1], Huade Zhao[3], Edward A Laws[4], Shuh-Ji Kao[1]*

[1]State Key Laboratory of Marine Environmental Science, Xiamen University, Xiamen, China

[2]Shenzhen Marine Environment Monitoring Center Station, Shenzhen, China

[3]National Marine Environmental Monitoring Center, Dalian, China

[4]Environmental Sciences Department, School of the Coast & Environment, Louisiana State University, USA

Correspondence to: Shuh-Ji Kao (sjkao@xmu.edu.cn)

Abstract

The general features of the N cycle in the sunlit region of the ocean ~~have been recognized~~are well known, but methodological difficulties have previously confounded simultaneous ~~quantitative~~ quantification of ~~information about multiple~~ transformation rates among the many different forms of N~~nitrogen pools~~, ~~i~~e.~~eg~~., ammonium (NH_4^+), nitrite (NO_2^-), nitrate (NO_3^-), and particulate/dissolved organic nitrogen (PN/DON)~~, are insufficient due to methodological difficulties~~. ~~Recent~~ However, recent advances in analytical ~~methods~~ methodology have made it possible to employ a convenient isotope labeling technique ~~for isotopic composition of oft-measured nitrogen species allowed us to establish a convenient isotope labelling method~~ to quantify ~~–~~*in situ* ~~dynamic~~ fluxes among oft-measured nitrogen species ~~flows for~~within the euphotic ~~water~~zone. ~~By a~~Addi~~ng~~tion of a single ^{15}N-labe~~l~~led NH_4^+ tracer and~~, we~~ monitor~~ing of~~~~ed~~ the changes ~~in~~ in the concentration~~s~~ and isotopic composition~~s~~ of the total dissolved nitrogen (TDN), PN, NH_4^+, NO_2^-, and NO_3^- pools allowed us to ~~trace~~ quantify the ^{15}N and ^{14}N ~~flows~~fluxes simultaneously. Constraints expressing the balance of ^{15}N and ^{14}N fluxes between the different N pools were expressed in the form of ~~Based on mass and isotope conservations of every individual pool as well as the whole system, we formulated matrix~~simultaneous equations~~, with~~ the unique solution of which via matrix inversion yielded the ~~to simultaneously derive multiple nitrogen transformation rates~~relevant N fluxes, ~~such as~~including rates of NH_4^+, NO_2^-, and NO_3^- uptake; ammonia oxidation; nitrite oxidation; DON release, and NH_4^+ uptake by

bacteria. Th~~is~~ ~~isotope~~ matrix inversion methodology that we used was designed specifically to analyze the results of incubations ~~for euphotic water column incubation~~ under simulated *in situ* conditions in the euphotic zone. ~~With~~ By taking into consideration ~~of multi~~simultaneous ~~flows~~uxes among multiple N pools, we minimized potential ~~biases~~ artifacts caused by non-targeted processes in traditional source-product methods. The proposed isotope matrix method ~~is~~ facilitates post-hoc analysis of data ~~convenient in terms of~~from on-deck incubation experiments ~~and post-hoc data analysis~~ and ~~is feasible~~can be used to probe effects of environmental factors (e.g., pH, temperature, and light) on multiple processes under ~~manipulated~~ controlled conditions.

Keywords

Ammonium oxidation, isotope, new production, nitrification, regenerated production

1. Introduction

Nitrogen (N), which is an essential element ~~in~~ for all organisms~~' metabolic processes~~, regulates productivity in the surface waters of many parts of the ocean (Falkowski, 1997; Zehr and Kudela, 2011; Casciotti, 2016). As a limiting nutrient in the euphotic zone, nitrogen rapidly interconverts among five major N compartments: particulate organic nitrogen (PN), dissolved organic nitrogen (DON), ammonium (NH_4^+), nitrite (NO_2^-), and nitrate (NO_3^-) (Fig. 1). ~~Quantitative information on~~Studies of the rates of transformation of N ~~rates~~ in the marine N-cycle ~~may advance~~have had a major impact on our current understanding of the coupling of autotrophic and heterotrophic processes involving carbon and nitrogen as well as the efficiency of the biological pump (Dugdale and Goering, 1967; Caperon et al., 1979; Harrison et al., 1992; Bronk and Glibert, 1994; Dore and Karl, 1996; Laws et al., 2000; Yool et al., 2007). Such information ~~would~~ has also facilitated evaluation of ecosystem functions. However, those studies have typically involved ~~the dynamic nature and complexity of the reactions involving nitrogen make it a difficult task to resolve the rates of multiple simultaneous nitrogen transformations. I~~inventory and isotope tracer methods that ~~have often~~ quantified the rates of only one or a few fluxes ~~been used to measure rate of specific process in previous studies~~ (Ward, 2008, 2011; Lipschultz, 2008 and references therein). The dynamic nature and complexity of the N cycle make simultaneous resolution of the rates of more than a few of the important fluxes a challenging task.

The inventory method (monitoring the change of substrate and/or product concentrations over time) ~~was~~ has often been used to determine the uptake rates of ammonium, nitrite, nitrate, and urea (McCarthy and Eppley, 1972; Harvey and Caperon, 1976; Harrison and Davis, 1977; Howard et al., 2007) and to examine the occurrence and rate of nitrification (Wada and Hatton, 1971; Pakulski et al., 1995; Ward, 2011). However, ~~unwanted~~ failure to account for other processes may bias the results. For example, the concentration of ~~substrate (~~ammonium~~)~~ ~~pool~~ is controlled simultaneously by ~~consumptions via~~removal via phytoplankton uptake (PN as the product), ~~nitrifier~~ nitrification (nitrite/nitrate as the product), and bacterial metabolism (operationally defined DON as product) and by additions via remineralization from heterotrophic bacterial metabolism, zooplankton excretion, and viral lysis. Similarly, the products ~~(NO_x^-) pool~~ of nitrification (NO_x^-) ~~is~~ may be simultaneously consumed ~~contemporarily~~ by phytoplankton ~~during incubation~~.

The ^{15}N-labeled tracer technique has been widely used as an ~~direct measure~~assay for specific nitrogen processes since the emergence of isotope ratio mass spectrometry (IRMS). For example, the addition of ^{15}N-labeled nitrate has been applied to estimate new production (Dugdale and Goering, 1967; Chen, 2005; Painter et al., 2014). Likewise, by incubating water to which $^{15}NH_4^+$ has been added, the nitrification rate ($^{15}NO_3^-$ as product; e.g. Newell et al., 2013; Hsiao et al., 2014; Peng et al., 2016) and ammonium uptake rate ($^{15}N_{PN}$ as product; e.g. Dugdale and Goering, 1967; Dugdale and Wilkerson, 1986; Bronk et al., 1994, 2014) can be measured~~, respectively, with~~via

incubations in the dark and light-, respectively~~incubation~~. However, the interpretation of isotope labe~~l~~ling experiments is confounded by the same ~~encounters similar bias~~ problems ~~in~~ as the inventory method, i.e., multiple processes that occur simultaneously ~~involving either~~impact the concentrations of ~~source~~ substrates ~~or~~ and products ~~terms~~ in the incubation bottle. In fact, ~~these~~ those transformations among pools have significant implications ~~in~~ for biogeochemical cycles. For instance, Yool et al. (2007) has synthesized available global data and ~~indicated~~ concluded that the fractional contribution of nitrate derived from nitrification to nitrate uptake can be as high as 19–33% in the euphotic zone. However, integration of the relevant rates over a light:dark cycle has been confounded by the fact that nitrate uptake rates ~~were~~ have typically been determined ~~under~~ during the photoperiod~~light conditions~~, ~~and~~ whereas nitrification rates have been ~~was determined under~~measured under dark conditions (e.g. Grundle et al., 2013~~),~~). Nitrate uptake may occur in the dark, but not necessarily at the same rate as in the light (Laws and Wong, 1978), and nitrification is inhibited by light (Dore and Karl, 1996). ~~which are not comparable in terms of their effects on these processes.~~ To ~~overcome this problem~~integrate rates over the light:dark cycle, 24-h incubations have been used to compensate for the diel cycle of light-sensitive processes (Beman et al., 2012). Yet, interpretation of the results of 24-h incubations may ~~cause calculation~~be confounded by artifacts due to ~~the interference from significant~~ transfers of ^{15}N and ^{14}N among pools. A new method is ~~needful~~ needed to ~~reconcile the~~

~~above-mentioned biases and the uncomparable parallel incubations~~overcome these problems.

Marchant et al. (2016) have reviewed recent methodological advances ~~in marine N-cycle studies~~ using ^{15}N-labeling substrates combined with nanoSIMS, FISH, or HISH in marine N-cycle studies. These methods provide qualitative information ~~for~~ about N transfers at the cellular and molecular level but do not ~~quantitative~~ quantify rates at the community level. Elskens et al. (2005) conducted ~~A~~ a comprehensive review of oft-used models for rate derivation ~~was conducted by Elskens et al. (2005), who~~and concluded that oversimplified models ~~would risk~~may lead to biased ~~when~~ results if their underlying assumptions are violated~~; . nevertheless~~However, overly complex models risk ~~could~~ misinterpreting ~~part of the~~ random noise as relevant processes. To address this concern, De Brauwere et al. (2005) ~~Therefore,~~proposed a model selection procedure ~~was subsequently proposed (De Brauwere et al., 2005)~~. More recently, Pfister et al. (2016) have applied an isotope tracer technique and mass conservation model ~~onto tidal pools study~~ to explore nitrogen flows among dissolved nitrogen pools (NH_4^+, NO_2^-~~-~~, and NO_3^-) in tidal ~~ponds~~ pools and found that benthic macrobiota played~~s~~ an important role in regulating remineralization ~~flow~~rates. They also ~~proved~~ found that ~~the~~ dilution effects significantly biased~~ed~~ the results obtained ~~by~~ with source-product models. ~~Nevertheless, f~~For the euphotic zone, where competing processes co-occur, an innovative and convenient method is needed to determine the

rates of multiple N fluxes from the results of ~~for on-deck~~simulated *in-situ* incubations ~~to measure *in situ* multiple N flows is needed~~.

In this study, we propose an "isotope matrix method". To avoid perturbations, the concentration of the tracer was limited to < 10% or 20 % of the substrate concentration, as suggested by previous researchers (Raimbault and Garcia, 2008; Middelburg and Nieuwenhuize, 2000; Painter et al., 2014). One single tracer, $^{15}NH_4^+$, was added ~~in~~to an incubation bottle to trace the ^{15}N flow among the nitrogen pools under simulated *in situ* conditions. Almost all the most fundamental processes in the N cycle can be quantified with this newly proposed method. To demonstrate the applicability of the method, we conducted incubation experiments ~~for~~ with low-nutrient water from~~in~~ the western North Pacific and ~~for~~ with high-nutrient coastal water off the southeastern China coast. ~~Thanks for~~ As a result of recent advances in the~~se~~ analytical methods for measuring the concentrations and isotopic compositions of various nitrogen species, we were able to use this isotope matrix method ~~becomes applicable~~ to quantify the *in situ*~~-~~ ~~dynamic~~ fluxes of ~~nitrogen flows for~~N in the euphotic zone~~water~~.

2. Isotope matrix method

2.1 Framework of the inter-connections among nitrogen pools

Figure 1 shows ~~In the oxygenated and well-lit euphotic zone,~~ the transformations of N among NH_4^+, NO_2^-, NO_3^-, PN, and DON in an aerobic euphotic zone~~are shown in Fig. 1~~. The PN ~~is~~ was operationally defined as the particulate organic nitrogen trapped on a GF/F filter (> 0.7 μm). Dissolved inorganic nitrogen (DIN) and DON ~~are~~ were

equated to the inorganic and organic nitrogen, respectively, in the dissolved fraction that passeds through a polycarbonate membrane with a 0.22 μm pore size. Since Because DON includes the N in numerous dissolved organic N compounds, including unidentified organics, urea, amino acids, amines, and amides, DON represents the "bulk" DON and is was calculated by subtracting the concentrations of NH_4^+, NO_2^-, and NO_3^- (DIN) from the total dissolved N (TDN).

We consider used two different types of schemesmodels in to analyze our methoddata: a low- nitrogen nutrient model to represent the open ocean and a high- nutrient model to represent estuarine and coastal environmentsitrogen (Fig. 1a and 1b). The low nutrient scheme is for the open ocean. In tThe high- nutrient scheme model, is for estuary and coastal environments where NH_4^+, NO_2^-, and NO_3^- were assumed tothree dissolved inorganic nitrogen species co-exist. Below, we describe tThe rationale for the twoof model structures is as follows for the two cases.

The consumption of reactive inorganic nitrogen (NH_4^+, NO_2^-, and NO_3^-) is dominated by photosynthetic uptake by phytoplankton (F1 and F4 in Fig. 1a; F1, F3, and F5 in Fig. 1b). Heterotrophic bacteria may also be play an important actors forrole in NH_4^+ assimilation (Laws, 1985), and was confirmed by studies later on (e.g.; Middelburg and Nieuwenhuize, 2000; Veuger et al., 2004). We took heterotrophic bacterial assimilation ofit NH_4^+ into account as well (F6 in Fig. 1a and F8 in Fig. 1b) to explore its importance. Though NO_2^- may be released during NO_3^- uptake (Lomas and Lipschultz, 2006), little NO_2^- production from NO_3^- was detected by (Santoro et al.,

(2013).~~,~~ ~~especially in high NH_4^+ estuary and coastal sea, n~~Nitrate assimilation may be inhibited in ~~oxygenated~~ aerobic ~~water~~ water, especially in estuaries and coastal seas where the NH_4^+ concentration is high, and in the absence of nitrate uptake, there is no release of ~~, subsequently, so is the~~ nitrite ~~release~~. Thus, ~~the~~ nitrite release was ignored in our model. Due to DIN assimilation by phytoplankton, the PN pool may increase, but DON may be released during assimilation (F5 in Fig. 1a and F7 in Fig. 1b) as ~~indicated by previous studies~~noted by ~~(~~Bronk et al.~~,~~ (1994~~;)~~, Bronk and Ward~~,~~ (2000~~;)~~, and Varela et al.~~,~~ (2005). ~~On the other hand, r~~The size of~~emineralization may refuel~~ the NH_4^+ pool is increased by remineralization (F2 in both Fig. 1a and 1b)~~.~~ ~~Meanwhile, ammonium pool is reduced~~and decreased by nitrification. The latter ~~process, which~~ consists of two basic steps: ~~the~~ ammoni~~a~~um oxidation by archaea/bacteria (AOA/AOB) to nitrite (F4 in Fig. 1b) and ~~the~~ nitrite oxidation to nitrate by nitrite-oxidizing bacteria (NOB) (F6 in Fig. 1b). Although recent studies have revealed a single microorganism that ~~may~~ can completely oxidize NH_4^+ to NO_3^- (comammox~~comammox~~) (Daims et al., 2015; van Kessel et al., 2015), ~~its~~ the importance of comammox in the marine environment remains unclear.

Specific mechanisms or processes such as grazing and viral lysis may alter the concentrations of NH_4^+, nitrite, and DON. However, the scope of this study is to determine the nitrogen ~~flows and exchanges~~fluxes among the often~~-~~measured and operationally defined nitrogen pools. ~~In this context, grazers and viruses belong to the operationally defined PN and DON pools, respectively~~The organisms that mediate the

relevant fluxes are not specifically included in the model. Thus, the results ance of specific process such as grazing and viral lysis has have been incorporated into the paradigm depicted in Fig.ure 1.

2.2 Analytical methods to determine the amounts of $^{15}N/^{14}N$ in various pools

To trace the ^{15}N movement among pools, our isotope matrix method couples the ^{15}N-labellinglabeling and inventory methods through by considering changes of both concentrations and isotopic compositions changes. Analytical methods to determine the concentrations and isotopic compositions of both high and low levels of inorganic/organic nitrogen are in most cases well established and have been reported elsewhere. We determined all of the mentioned relevant concentrations and isotopic compositions with the exception of the isotopic composition of NH_4^+.

Concentrations of NH_4^+ higher than 0.5 μM were measured manually by using the colorimetric phenol hypochlorite technique (Koroleff, 1983). Nanomolar NH_4^+ concentrations were measured by using the fluorometric o-phthaldialdehyde (OPA) method (Zhu et al., 2013). Concentrations of NO_2^- and of NO_x^- (NO_2^- + NO_3^-) were determined with the chemiluminescence method following the protocol of Braman and Hendrix (1989). The detection limits of NO_2^- and NO_x^- were both ~ 10 nmol L^{-1}, and the corresponding relative precision was better than 5% within the range of concentrations that we measured. By using persulfate as an oxidizing reagent, we oxidized TDN and PN separately to nitrate (Knapp et al., 2005) and then measured the nitrate by using the analytical method for NO_x^- described above.

213 We determined the $\delta^{15}N$ of NO_2^- with the azide method by following the detailed
214 procedures in McIlvin and Altabet (2005). The $\delta^{15}N$ of NO_x^- was determined by using a
215 distinct strain of bacteria that lacked N_2O reductase activity to quantitatively convert
216 NO_x^- to nitrous oxide (N_2O), which we then analyzed by IRMS (denitrifier method;
217 (Sigman et al., 2001; Casciotti et al., 2002). The isotopic composition of NO_3^- was
218 determined from isotope mass balance (NO_x^- minus NO_2^-) or measured by the
219 denitrifier method after eliminating preexisting NO_2^- with sulfamic acid (Granger and
220 Sigman, 2009). To determine the $\delta^{15}N$ of TDN and PN, both species were first
221 converted to NO_3^- with the denitrifier method, and then the $\delta^{15}N$ of the NO_3^- was
222 determined as described above. The detection limit of $\delta^{15}N_{PN}$ can be reduced to the
223 ~~nanomole~~ nanomolar level (absolute amount of nitrogen), which is significantly lower
224 than ~~that~~ the detection limit ~~by~~ using high temperature combustion with an elemental
225 analyzer connected to IRMS.

226 The most popular way to determine the N isotopic composition of NH_4^+ is the
227 "diffusion method", which involves conversion of dissolved NH_4^+ to NH_3 gas by
228 raising the sample pH to above 9 with magnesium oxide (MgO) and subsequently
229 trapping the gas quantitatively as $(NH_4)_2SO_4$ on a glass fiber (GF) filter; the isotope
230 ratios of the $^{15}N/^{14}N$ are then measured using an ~~coupled~~ elemental analyzer coupled
231 with an IRMS (Holmes et al., 1998; Hannon and Böhlke, 2008). Alternatively, after
232 removing the preexisting NO_2^- from the seawater samples using sulfamic acid, NH_4^+ is
233 first quantitatively oxidized to NO_2^- by hypobromite (BrO^-) at pH ~12 (BrO^- oxidation

method), and the protocol of McIlvin and Altabet (2005) is then used to reduce the NO_2^- to N_2O (Zhang et al., 2007). Unfortunately, neither of these methods has been established in our lab yet. The isotope matrix method requires the isotopic composition of NH_4^+ as well, but this requirement can be circumvented by making certain assumptions, as illustrated in our case studies below.

We estimated the amount of ^{14}N and ^{15}N atoms in every individual pool for which we knew the concentration and $\delta^{15}N$ ($\delta^{15}N$ ‰ = $[(R_{sample} - R_{atmN2})/R_{atmN2}] \times 1000$). By assuming the ^{15}N content of standard atmospheric nitrogen to be 0.365% (Coplen et al., 1992), we calculated R_{sample} ($^{15}N/^{14}N$). By defining r_{sample} as $^{15}N/(^{14}N+^{15}N)$, we directly derived the ^{15}N and ^{14}N concentrations of all forms of N, with the exception of NH_4^+ and DON. The r value of the NH_4^+ was assumed to equal either its initial value or an arbitrarily chosen fraction thereof, and the ^{15}N and ^{14}N content of the NH_4^+ was then determined.

2.3 Formation of matrix equations

In this isotope matrix method, we added a limited amount of $^{15}NH_4^+$ into incubation bottles at the very beginning and then monitored the changes of ^{15}N and ^{14}N in the measured pools every ~~a~~ few hours. We assumed isotopic mass balance at every time point in the incubation bottle. In other words, the sum~~s~~ of the variations in the total N, ^{15}N, and ^{14}N concentrations were zero for any time interval. ~~We assumed no fractionation between ^{15}N and ^{14}N for all the transfer reactions among the pools.~~ The fluxes of ^{15}N and ^{14}N were therefore equal to the total flux multiplied~~, respectively,~~ by

$r_{substrate}$ and $(1 - r_{substrate})$, respectively. ~~Note that w~~Although we~~e~~ did not consider isotope fractionation, ~~though~~ it could have been ~~easily be~~ introduced into the equations ~~if necessary, i.e.,~~by dividing the ^{14}N flux by ~~α (~~the ratio of the specific rate constants of ^{14}N ~~to~~ and ^{15}N~~)~~ to obtain~~,~~ ~~and~~ the flux of ^{15}N ~~is obtained~~. ~~Below, we illustrated equations for the two model cases.~~

According to mass balance, the net changes of the ^{15}N (or ^{14}N) concentration of an individual N pool in a ~~certain~~ time interval are determined by the inflow and outflow of ^{15}N (or ^{14}N) (see Fig. 1 and Eqs. 1–14 below). In the low-nitrogen case, the changes of the ^{15}N concentrations of the NH_4^+, NO_x^-, and PN pools were expressed by Eq. 1, 2, and 3, respectively. Similarly, the temporal dependence of ^{14}N-NH_4^+, ^{14}N-NO_x^-, and ^{14}N-PN were expressed by Eq. 4, 5 and 6, respectively. The mean rate of change ~~in~~ of the nitrogen pool, i.e. the left side of ~~the~~ each equation, was determined from the data at time zero (t0) and the first time point (t1). For example, when the sampling time interval ~~is~~ was short, $\Delta[^{14}NH_4^+]/\Delta t$ at the first time point was approximately $\{[^{14}NH_4^+]_{t1} - [^{14}NH_4^+]_{t0}\}/(t1 - t0)$ where the subscripts indicate the times at which the concentrations were measured. The r value ~~applied~~ in ~~the~~ each equation ~~for substrate~~ was the average of the r values for the pool at time zero and the first time point ~~after that for measured pool~~.

$$\frac{\Delta\left[{}^{15}NH_4^+\right]}{\Delta T} = \overline{F_2} \times 0.00366 - \overline{F_1} \times \overline{r_{NH_4^+}} - \overline{F_3} \times \overline{r_{NH_4^+}} - \overline{F_6} \times \overline{r_{NH_4^+}} \quad (1)$$

$$\frac{\Delta\left[{}^{15}NO_x^-\right]}{\Delta T} = \overline{F_3} \times \overline{r_{NH_4^+}} - \overline{F_4} \times \overline{r_{NO_x^-}} \quad (2)$$

$$\frac{\Delta\left[{}^{15}PN\right]}{\Delta T} = \overline{F_1} \times \overline{r_{NH_4^+}} + \overline{F_4} \times \overline{r_{NO_x^-}} - \overline{F_5} \times \overline{r_{PN}} \quad (3)$$

$$\frac{\Delta\left[{}^{14}NH_4^+\right]}{\Delta T} = \overline{F_2} \times (1 - 0.00366) - \overline{F_1} \times (1 - \overline{r_{NH_4^+}}) - \overline{F_3} \times (1 - \overline{r_{NH_4^+}}) - \overline{F_6} \times (1 - \overline{r_{NH_4^+}}) \quad (4)$$

$$\frac{\Delta\left[{}^{14}NO_x^-\right]}{\Delta T} = \overline{F_3} \times (1 - \overline{r_{NH_4^+}}) - \overline{F_4} \times (1 - \overline{r_{NO_x^-}}) \quad (5)$$

$$\frac{\Delta\left[{}^{14}PN\right]}{\Delta T} = \overline{F_1} \times (1 - \overline{r_{NH_4^+}}) + \overline{F_4} \times (1 - \overline{r_{NO_x^-}}) - \overline{F_5} \times (1 - \overline{r_{PN}}) \quad (6)$$

~~In this study, we conducted a~~The time series ~~monitoring for over~~in this study lasted for 24 hours~~, .~~ ~~however~~However, we ~~took~~ used only the first two time points for the rate calculations ~~since such~~because we felt those rates ~~derivations might~~would be ~~be more~~ closest to the instantaneous *in situ* rates ~~in~~ of the original ~~environments~~samples. ~~Note: researchers may apply~~Although ~~this~~ the isotope matrix method ~~onto~~ may be applied to longer time intervals, ~~however,~~ rates may vary as a result of substrate consumption and/or community change~~, .~~ Relatively short~~er~~-term incubations ~~is~~ are therefore advisable ~~suggested~~ (see below).

~~Since~~ Because the total number of equations and unknowns are equal, a unique solution ~~therefore~~ can be obtained via matrix ~~solution~~ inversion for the low~~-~~-nutrient model.

In high~~-~~-nutrient cases, ~~similar~~analogous~~ly,~~ equations (Eqs. 7~~–~~14) can be constructed ~~by~~ to describe the ~~using transformations among~~fluxes between NH_4^+, NO_2^-, NO_3^-~~-~~, and PN (Fig. 1b).

$$\frac{\Delta\left[{}^{15}NH_4^+\right]}{\Delta T} = \overline{F_2}\times 0.00366 - \overline{F_1}\times\overline{r_{NH_4^+}} - \overline{F_4}\times\overline{r_{NH_4^+}} - \overline{F_8}\times\overline{r_{NH_4^+}} \quad (7)$$

$$\frac{\Delta\left[{}^{15}NO_2^-\right]}{\Delta T} = \overline{F_4}\times\overline{r_{NH_4^+}} - \overline{F_3}\times\overline{r_{NO_2^-}} - \overline{F_6}\times\overline{r_{NO_2^-}} \quad (8)$$

$$\frac{\Delta\left[{}^{15}NO_3^-\right]}{\Delta T} = \overline{F_6}\times\overline{r_{NO_2^-}} - \overline{F_5}\times\overline{r_{NO_3^-}} \quad (9)$$

$$\frac{\Delta\left[{}^{15}PN\right]}{\Delta T} = \overline{F_1}\times\overline{r_{NH_4^+}} + \overline{F_3}\times\overline{r_{NO_2^-}} + \overline{F_5}\times\overline{r_{NO_3^-}} - \overline{F_7}\times\overline{r_{PN}} \quad (10)$$

$$\frac{\Delta\left[{}^{14}NH_4^+\right]}{\Delta T} = \overline{F_2}\times(1-0.00366) - \overline{F_1}\times(1-\overline{r_{NH_4^+}}) - \overline{F_4}\times(1-\overline{r_{NH_4^+}}) - \overline{F_8}\times(1-\overline{r_{NH_4^+}}) \quad (11)$$

$$\frac{\Delta\left[{}^{14}NO_2^-\right]}{\Delta T} = \overline{F_4}\times(1-\overline{r_{NH_4^+}}) - \overline{F_3}\times(1-\overline{r_{NO_2^-}}) - \overline{F_6}\times(1-\overline{r_{NO_2^-}}) \quad (12)$$

$$\frac{\Delta\left[{}^{14}NO_3^-\right]}{\Delta T} = \overline{F_6}\times(1-\overline{r_{NO_2^-}}) - \overline{F_5}\times(1-\overline{r_{NO_3^-}}) \quad (13)$$

$$\frac{\Delta\left[{}^{14}PN\right]}{\Delta T} = \overline{F_1}\times(1-\overline{r_{NH_4^+}}) + \overline{F_3}\times(1-\overline{r_{NO_2^-}}) + \overline{F_5}\times(1-\overline{r_{NO_3^-}}) - \overline{F_7}\times(1-\overline{r_{PN}}) \quad (14)$$

~~Again, a~~A unique solution can again be obtained via matrix inversion ~~since~~ because the number~~s~~ of equations and unknowns are equal.

In the above matrix equations, the value of r_{NH4+}, which we did not measure in this study, ~~is~~ was ~~necessary for the~~needed to obtain a solution. ~~Here~~ To address this issue, we ~~set~~ assumed various degrees of remineralization to test the effect of isotope dilution (NH_4^+ addition) ~~in~~ on our ~~experimental cases~~calculated fluxes. We reduced r_{NH4+} values ~~at a constant reduction rate and the total reduction of r_{NH4+} was 0%, 1%, 10%, 20% and~~

50% for the full time spanof the 24-h incubation. (The r_{NH4+} of for remineralization (F2) is was assumed to be constant (0.00366) and equal constant rates that led to total reductions of r_{NH4+} by 0%, 1%, 10%, 20%, or 50% by the end). The value of F2 coupled with given the assumed r_{NH4+} values allowed us to resolve rates under different remineralization conditionsscenarios, and the derived F2 was introduced into a STELLA model for extrapolation purposess (see below). We compared the observed and remineralization-associated simulations to reveal elucidate the effect of remineralization on the calculated rates measure for the time series incubations.

2.4 Validation by STELLA

As the aforementioned, tThe "instant rate"initial rates are of particular interest because they are presumably most similar to the *in situ* rates at the time the sample was collected at the original condition is what researchers pursue. Note that the use ofThe initial rate is here distinguished "instant" here is just to make it distinguishable from rates derived from the longer time incubations that extended beyond time point t1or more than two time points. To evaluate the applicability of the matrix-derived instant initial rate, here we applied used STELLA 9.1.4 software (Isee systems, Inc.) to construct box models that were consistent with the scenarios depicted in Fig.ure 1. The constructed STELLA model contained two modules (Figs. S1 and S2), one for ^{15}N and the other for ^{14}N. The connection between these two modules was were connected through the ^{15}N atom % (rN), which was a measured parameter measured in the incubation experiment. The A model started to run was initialized with thesse measured

~~initial~~ values ~~for~~ of the nitrogen pools at time zero, and the model then ~~to~~ projected ~~continuous~~ the ~~changes~~ values of ~~corresponding~~ those ~~nitrogen~~ pools as a continuous function of time. ~~Since~~ Because the rates ~~numbers~~ based on the first two time points ~~may~~ might not accurately represent the behavior of the system throughout ~~not guarantee a good performance for~~ the full time course due ~~to system variation~~, for example, ~~i.e.,~~to changes in substrate concentrations and the composition of the ~~microorganism~~ microbial community, ~~we took~~ this ~~model practice (~~extrapolation using the initial rates~~)~~ ~~as~~ amounted to a test of the hypothesis that the rates did not change~~a validation~~.

~~In this study, w~~We assumed ~~the~~ first~~-~~order reaction kinetics ~~for~~ in both the low-nutrient and high-nutrient cases.~~,~~ ~~thus, t~~The initial rate constant "k" ~~can~~ could therefore be derived ~~via~~ by dividing the matrix-derived flux F by $\bar{C}$, ~~(~~the average substrate concentration ~~of~~ during the first two time points~~)~~. After ~~setting the initial~~the concentrations of ^{15}N and ^{14}N were initialized ~~to~~ in every pool, the model ran for 24 h ~~according to~~using the matrix-derived short-term k values. As depicted in Fig~~ure~~ 1, all ~~these~~ monitored N pools ~~are~~ were regulated by F, which ~~is~~ was assumed to be concentration dependent ~~according to our assumption~~ (Figs. S1 and S2). The output of the model ~~includes~~ included the time courses of the ^{15}N and ^{14}N concentrations and the ^{15}N atom % (r_N) of each N species. Through this ~~comparison~~analysis, we could observe the ~~course~~ temporal evolution of the isotopic composition ~~in~~ of the various N pools.

2.5 Study sites and incubation experiments

~~Incubation~~ The incubation experiments were conducted in two environments with very different nutrient levels. The low~~-~~nutrient ~~case~~ study was conducted on-deck of the R/V Dongfanghong 2 on a cruise to the Western North Pacific (WNP) (33.3 °N, 145.9 °E) in the spring of 2015. The site ~~for~~ of the high~~-~~nutrient ~~case~~ study ~~is~~ was ~~in the~~ Wuyuanwan Bay (WYW) (24.5 °N, 118.2 °E) in the southern coast of China.

The water samples at the WNP station were collected using a 24-bottle rosette sampler. The sampling depth was 25 m, at which the ~~with moderate~~ light intensity was ~~(~~12% of the surface ~~water~~ irradiance~~)~~. Two pre-washed 10-L polycarbonate carboys (Nalgene, USA) were used for the incubation. A total of 1.5 mL of 200 μM ^{15}N-labe~~l~~led NH_4Cl tracer~~s~~ containing 98 atom % ^{15}N (Sigma-Aldrich, USA) was injected into each incubation bottle separately to achieve a final concentration of 30 nM. ~~Incubation~~ The incubation was carried out immediately with a constant simulated light intensity of ~~(~~35 μmol ~~E~~ photons m^{-2} s^{-1}~~)~~ in a thermostatic incubator (GXZ-250A, Ningbo) at the *in situ* temperature.

The WYW station ~~is~~ was ~~an~~ located in the inner bay, where the tide was ~~with a regular~~ semidiurnal ~~tide~~. ~~As a coastal bay,~~ Wuyuanwan, a coastal bay, suffers from the same anthropogenic influences that cause eutrophication ~~result in high nutrient concentrations analogous to~~in other coastal ~~zones~~ areas ~~in~~ of China. However, the bay water is ~~still~~ well ventilated and constantly saturated with dissolved oxygen due to tidally induced water exchange. It is an ideal ~~research~~ site to study the dynamic transformations that characterize ~~processes of~~ the coastal nitrogen cycle.

The WYW samples were taken on 19 January~~,~~ 2014 from water depths of 0.3 m and 2.3 m, where the ~~, respectively, with a~~ light ~~intensity~~ intensities ~~of~~ were 80~~-~~% and 2%, respectively, of the surface water irradiance. Duplicate water samples were collected ~~for~~ from each depth by using submersible pump ~~into~~ to fill pre-washed 10-L polycarbonate bottles (Nalgene, USA). ^{15}N-labeled NH_4Cl (98 atom % ^{15}N, Sigma-Aldrich, USA) was added to the incubation bottles ~~with~~ to a final concentration of 1 μM (~4~~-~~% of the ambient concentration). The incubations were carried out immediately in the field. Neutral density ~~-~~screens that ~~allows~~ allowed 80% and 2% light penetration ~~was applied, respectively~~were used to simulate the light intensities at 0.3 m and 2.3 m, respectively~~, for incubation bottles of shallow and deep samples~~. The temperature was maintained at ~13.7 ℃ by continuously ~~pumped~~ pumping seawater through the ~~flow~~incubators.

The ~~Sample~~ sample ~~of~~ at the first time point (t0) was taken immediately after tracer addition. Subsequent samples were taken at approximately 2–4 h intervals ~~–~~for DIN and PN analyses. An aliquot of 200 mL was filtered through a 47-mm polycarbonate membrane filter with a 0.22 μm pore size (Millipore, USA~~),~~). ~~and t~~The filtrates were frozen at –20 ℃ for chemical analyses in the lab. Particulate matter was collected by filtering 500 ml seawater through pre-combusted (450 ℃ for 4 h) 25 mm GF/F filters (Whatman, GE Healthcare, USA)~~, under~~ at a pressure of <100 mm Hg. The GF/F filters were freeze-dried and stored in a desiccator prior to ~~for~~ analysis of PN concentrations and ^{15}N atom %~~isotopes~~.

3. Results

3.1 Ambient conditions and initial concentrations

The water temperature and salinity at a depth of 25 m ~~of~~ in the WNP ~~low nutrient case from 25m was~~were 18.4 ℃ and 34.8, respectively. The dissolved oxygen (DO) was 7.3 mg L^{-1}. The concentrations of NH_4^+, NO_x^-, and phosphate ~~was~~ were 113 ± 5 nmol L^{-1}, 521 ± 18 nmol L^{-1} and 74 ± 2 nmol L^{-1}, respectively. ~~The fact that the N/P ratio was lower less than 16, indicated thating the system is was N limited.~~

The water temperature and salinity ~~of the~~throughout the water column of the WYW ~~whole water column for high nutrient case was~~were 13.5 ± 0.1 ℃ and 29.5 ± 0.1, respectively. The DO saturation fell in the range~~d~~ 135~~–~~–140%. The concentrations of nitrogenous species were relatively high. ~~with~~ The inorganic nutrient concentrations ~~of~~ were 30.9 ± 0.7 μmol L^{-1} for NO_3^-, 22.3 ± 4.3 μmol L^{-1} for NH_4^+, 5.4 ± 0.2 μmol L^{-1} for NO_2^-, and 1.5 ± 0.1 μmol L^{-1} for phosphate. ~~, and~~ The PN concentration was 9.3 ± 0.7 μmol L^{-1}. ~~for PN. Phosphate was 1.5 ± 0.1 μmol L^{-1}.~~

3.2 Time-courses of incubations

3.2.1 Low nutrient case in the WNP

The observed ~~variation~~ patterns of change ~~for~~ of the bulk NH_4^+, NO_x^-, PN, and TDN concentrations and the $\delta^{15}N$ of NO_x^- and PN during the incubation are shown in Figure 2. Concentrations of NH_4^+ and NO_x^- decreased rapidly from 143 ± 5 to 48 ± 5 nM and 521 ± 18 to 127 ± 11 nM, respectively (Figs. 2a and 2b). In contrast, the PN concentration increased from 437 ± 9 to 667 ± 14 nM (Fig. 2c), and the TDN

concentration remained stable, with an average of 6511 ±209 nM (Fig. 2d). ~~Opposite~~ In contrast to ~~to~~ the trend of NO_x^- concentration, $\delta^{15}N\text{-}NO_x^-$ increased from 8.9 ±0.2 to 171 ±2 ‰ (Fig. 2e). In addition, $\delta^{15}N$-PN exhibited great changes, increasing from 46.8 ±0.2 to 6950 ±314 ‰ (Fig. 2f).

3.2.2 High nutrient case in the WYW ~~s~~

The time-series of observational parameters for samples from depths of 80% and 2% ~~sPAR~~ of surface PAR (sPAR) exhibited similar ~~variation~~ trends during the incubation (Fig. 3). During the course of the incubation, NH_4^+ decreased significantly and continuously from 26.6 ±0.1 (initial concentration) to 17.4 ±0.1 μmol L^{-1}. ~~with a~~The mean reduction rate ~~of~~ was 0.63 μmol L^{-1} h^{-1} ~~for~~ for the 80% sPAR sample (Fig. 3a). ~~Compared with that of 80% sPAR,~~The NH_4^+ concentration of 2% sPAR sample decreased ~~slower~~ more slowly from 24.6 ±0.1 (initial concentration) to 18.2 ±1.0 μmol L^{-1} with a mean reduction rate of 0.47 μmol L^{-1} h^{-1} (Fig. 3a). NO_3^- in 80% and 2% sPAR samples decreased from 30.1 ±0.1 to 28.3 ±0.1 μmol L^{-1} and from 31.1 ±0.1 to 29.7 ±0.1 μmol L^{-1}, respectively (Fig. 3c). Overall, the nitrate reduction rates were much lower than ~~that of~~the NH_4^+. reduction rates. Compared to nitrate, NO_2^- displayed even slower rates of declin~~ing trends~~e, yet ~~with~~ the rate was significantly higher ~~rate for~~ at 80% sPAR ~~sample relative to that of~~than at 2% sPAR ~~sample~~ (Fig. 3b). Similar to the low nutrient case, PN increased steadily from 8.8 ±0.1 to 17.7 ±0.9 μmol L^{-1}, with a mean rate of 0.61 μmol L^{-1} h^{-1} ~~for~~ at 80% sPAR ~~sample~~ and from 9.9 ±0.1 to 16.0 ±2.0 μmol L^{-1} with a mean rate of 0.44 μmol L^{-1} h^{-1} ~~in~~ at 2% sPAR (Fig. 3d). The rates of

increase ~~rates in~~of the PN concentration were very close to the rates of decrease ~~rates~~ of NH_4^+~~-~~, the ~~indicating~~ indication being that ammonium was the major nitrogen source for growth. The TDN concentration decreased from 78.7 ± 1.6 to 68.4 ± 0.1 μmol L^{-1} and ~~form~~ from 72.8 ± 2.5 to 67.1 ± 0.8 μmol L^{-1} at ~~for~~ 80% and 2% sPAR ~~samples~~, respectively (Fig. 3e).

The $\delta^{15}N\text{-}NO_2^-$ increased from –9.0 ± 0.1 to 12.1 ± 0.1 ‰ and from ~~–~~–8.8 ± 0.1 to 23.3 ± 0.6 ‰ ~~in~~ at 80% and 2% sPAR ~~incubation~~, respectively (Fig. 3g~~); ~~). ~~Since~~ Because the nitrate pool was relatively large, the values of $\delta^{15}N\text{-}NO_3^-$ ranged from 6.8 to 10.1 ‰ with no significant trend over time (Fig. 3h). In addition, $\delta^{15}N$-PN increased from 14.8 ± 0.3 to 3078 ± 180 ‰ and from 15.0 ± 0.5 to 2738 ± 66 ‰ ~~for~~ at 80% and 2% sPAR ~~sample~~, respectively (Fig. 3i). These significant changes in both the concentration and isotopic composition~~s~~ of the nitrogen pools over time ~~suggested~~ suggests that there were significant movements of nitrogen ~~transformed significantly~~ among pools and that the labe~~l~~led ^{15}N in the NH_4^+ ~~flowed~~ moved throughout the system, with the exception of nitrate.

3.3 Solutions of the matrix equation and STELLA extrapolation

3.3.1 Low nutrient case

The matrix-derived rate constants (ki) and rates (Fi) are shown in Table 1(A) and 1(B), respectively. Under the no remineralization condition (i.e. r_{NH4+} decreased 0% within 24 hours), ~~the~~ NO_x^- uptake (k4 = 0.059 h^{-1}; F4 = 27.2 nmol L^{-1} h^{-1}) was the highest among all forms of inorganic nitrogen in terms of flux, followed by NH_4^+

uptake (k1 = 0.038 h^{-1}; F1 = 4.9 nmol L^{-1} h^{-1}) and DON release (k5= 0.024 h^{-1}; F5 = 11.5 nmol L^{-1} h^{-1}). NH_4^+ uptake by bacteria (k6 = 0.007 h^{-1}; F6 = 1.0 nmol L^{-1} h^{-1}) was much lower than that by phytoplankton. The rate constant for nitrification (k3 = 0.0005 h^{-1}) was the lowest among all fluxes (F3 = 0.07 nmol L^{-1} h^{-1}).

By introducing the initial ^{15}N and ^{14}N concentrations of NH_4^+, NO_x^-, PN, and DON and the calculated rate constants (k1 to k6) into STELLA (Fig. S1), we obtained a full time courses for all parameters (Fig. 4). Generally, the model outputs fitted well with the measured values, except for the last time point for PN, the associated ^{15}N concentration, $\delta^{15}N$, and r_N (Figs. 4 c, k and o). ~~In general,~~The fact that the rates ~~of~~ during the first time interval ~~can well~~ generally predicted rather well the ~~following~~ ~~up~~subsequent observations~~,~~ demonstrated~~ing~~ a good predictive performance ~~by~~ ~~using~~with the matrix method ~~instant~~ initial rate. ~~Since~~ Because the concentrations of both ~~substrates, e.g.,~~ ammonium and NO_x^- were~~,~~ ~~fitted~~ described well ~~within~~ during the 24~~-~~h experiment~~ours~~, the extra ~~non-fitted~~ PN that was not well described in observations after ~~the time point of~~ 12 hours likely ~~indicated~~ reflected the ~~participation~~ influence of an additional nitrogen source, i.e., dissolved organic nitrogen that was utilized by phytoplankton (see discussion below) when inorganic nitrogen reached threshold levels (Sunda and Ransom, 2007).

In the~~se~~ test runs ~~of regeneration~~ with r_{NH4+} reduction by a total ~~amount~~ of 1~~-~~%, 10~~-~~%, 20~~-~~% and 50~~-~~%, we found that the NH_4^+ consumption rates (k1 and k6) increased as the regeneration (k2) increased (Table 1). As indicated in previous studies, such

regeneration-induced isotope dilution indeed altered the original results (Table 1 and Fig. 4). ~~More s~~Specifically, greater NH_4^+ regeneration resulted in larger differences between the~~se~~ three PN-associated values (^{15}N-PN, δ^{15}N-PN, and r_{PN}) and the STELLA-projected data (Figs. 4 c, k and o). ~~Meanwhile, t~~The dilution effect was more significant after 12 hours of incubation. ~~On the other hand~~In contrast, the effect of r_{NH4+} on ~~NO_x^- associated~~ parameters associated with NO_x^- was trivial (Figs. 4 b, f, j, n and r). The comparison between the simulation and observation suggested that NH_4^+ regeneration needs to be considered for PN (i.e., uptake) when the remineralization rate is high and the incubation ~~prolongs~~is longer than 12 hours. Besides remineralization, ~~offsets~~ discrepancies along the time course might possibly be ~~induced~~ caused by ~~by~~ changes in the ~~community change~~ composition of the microbial community as the incubation ~~prolongs~~continues.

3.3.2 High nutrient cases

The results at~~of~~ 80% sPAR and 2% sPAR ~~under~~ on the assumption of a fixed r_{NH4+} are shown in Table 2(A) and 2(B), respectively. For the ~~high light sample (~~80 ~~%~~% sPAR sample~~)~~, the NH_4^+ uptake by phytoplankton (F1, 397 nmol L^{-1} h^{-1}) and by bacteria (F8, 282 nmol L^{-1} h^{-1}) were much higher than the other rates and were followed by the NO_3^- uptake rate (F5, 149 nmol L^{-1} h^{-1}). The NO_2^- uptake (F3) rate was 29 nmol L^{-1} h^{-1}, much lower than that of NH_4^+ and NO_3^- ~~uptake~~. The ammonia oxidation rate (F4) was 0.4 nmol L^{-1} h^{-1}, and the nitrite oxidation rate (F6) was zero (Table 2A). ~~Since~~ Because this incubation was conducted in winter with low

temperature and ~~under~~ at 80% sPAR~~ light conditions~~, low rates of ammonium and nitrite oxidation were reasonable because both nitrifiers and NOB are sensitive to light (e.g. Olson, 1981a, 1981b; Horrigan et al., 1981; Ward, 2005; Merbt et al., 2012; Smith et al., 2014). The DON release rate by phytoplankton (F7) was zero in this case.

In comparison, all the rates ~~in the condition of~~at 2% sPAR showed a very similar pattern (Table 2B). The only difference was that all the uptake rates were lower ~~for~~ ~~the~~at 2% sPAR, except for ammonia oxidation, which was higher in the low light.

By introducing initial concentrations and calculated rate constants (k1–k8) into the STELLA model (Fig. S2), we obtained ~~successive variations~~a time series of ^{15}N and ^{14}N concentrations and the r_N values for ~~of~~ NH_4^+, NO_2^-, NO_3^-, PN and DON ~~over time~~ (Fig. 5). In general, the modeled and measured values remained consistent throughout the 15-h incubation, demonstrating the capability of the isotope matrix method.

Similar to the low-nutrient case, we evaluated the effect of regeneration (see Table 2 and Fig. 5A and 5B). ~~Since~~ Because ammonium uptake was the dominant process, ~~the alteration~~changes of the PN pool were~~as~~ more significant in comparison with the other pools (Figs. 5 d, n and s). We found again that~~,~~ as F2 increased, F1 and F8 increased to maintain a constant reduction of the measured NH_4^+ concentration (Table 2). Similar to the low-nutrient case, as regeneration increased, the projected course of ^{15}N-PN deviated more from observations, and the turning point also appeared earlier, resulting in a larger curvature of r-PN and $\delta^{15}N$-PN (Fig. 5d and 5s). This

modeling exercise confirmed the influence of the isotope dilution effect.; However, the effect was is insignificant in the early stage part of the incubation.

4. Discussion

4.1 Method comparisons

4.1.1 Model structure and rate derivation

The most widespread ^{15}N model was proposed by Dugdale and Goering (1967), who assumed the isotopic and mass balances in the particulate fraction, the result being in the commonly used formula equation for nitrogenous nutrient uptake. Dugdale and Wilkerson (1986) modified their rate equations further and highlighted the importance of short-term incubations. Although short-term incubation was requested, Collos (1987) demonstrated that anthe formula equation based on the concentration of particles at the end of the experiment, rather than at the beginning, wasis more reliable when more than one N source wasare simultaneously incorporated by the phytoplankton population. That is, the equation by Collos (1987) corrected for the bias caused by use of unlabeled multiple N utilizationsources.

Different fromUnlike the above- mentioned equations, Blackburn (1979) and Caperon et al. (1979) proposed ^{15}N isotope dilution models based on the substrate rather than the product. By measuring the isotope values and concentrations of the substrate, (e.g. NH_4^+), and then both NH_4^+ consumptions (DON and/or PN as product) and regeneration rates can be obtained. Glibert et al. (1982) further modified the

isotope dilution method and calculated the uptake rate into the PN fraction by substituting the exponential average of r_{NH4+} at the beginning and at the end of an incubation to correct for the isotope dilution ~~existing~~ in the model of Dugdale and Goering (1967). ~~Besides~~ Despite the methodological improvements, imbalance was often observed between the substrate reduction and the increase in the particulate phase in field studies. Laws (1985) introduced a new model that~~with~~ considered~~ation of~~ the imbalance and calculated the "net uptake rate" (into PN). Later on, Bronk and Glibert (1991) revised Law~~'~~s' model on the basis of the model proposed by Glibert et al. (1982) to calculate the "gross uptake rate" (substrate incorporation into ~~PON~~ particulate organic nitrogen plus DON). ~~Overall speaking,~~ N~~n~~one of the above models considered the mass balance at the whole system scale. Although rates were obtained via analytical solutions, the bias potential due to multiple fluxes~~ows~~ was not completely resolved.

To ~~solve multiple co-occurring N processes~~address this problem, Elskens et al. (2002) formulated a new model that takes into account multiple co-occurring N fluxes in a natural system~~,~~. The model contain~~s~~ing 3n + 1 equations and an equal number of flux rates, where ~~(~~n ~~stands for~~is the number of labe~~l~~led N substrate~~s) and 3n+1 flux rates, by taking multiple co-occurring N fluxes in natural system into account~~. ~~Approximate~~ The rates in their model were ~~resolved~~ estimated using ~~by~~ a weighted least squares technique. ~~Additionally,~~ Elskens et al. (2005) subsequently created a process-oriented model (PROM) that account~~ing~~ for as many N processes as

needed to quantify how specific underlying assumptions affected the ~~estimation~~ behavior of the estimates of all the above-mentioned models. The authors concluded that uncertainties may increase as the incubation is ~~prolongs~~ prolonged and that oversimplified models may risk bias when their underlying assumptions are violated. The most recent attempt to resolve simultaneous N processes was conducted by Pfister et al. (2016), who ~~applied~~ used parallel incubations (^{15}N labe~~l~~led NH_4^+ and NO_3^-) in tidepools to measure multiple flows among benthic N, ammonium, nitrite, and nitrate ~~pools~~. In their experiment, six differential equations ~~(with seven unknowns)~~ were constructed ~~basing~~ based on mass and isotope balances and solved by using the ODE function of the R language. ~~Since~~ Because the N content of benthic algae ~~were~~ was not measured due to sampling ~~difficulty~~ difficulties ~~in sampling~~ and spatial heterogeneity ~~in~~ of biomass, a mass balance at the whole system scale ~~mass balance cannot~~ could not be ~~reached~~achieved~~;~~. Specifically, ~~thus,~~ the ~~flux~~ rate of DON release ~~cannot~~ could not be ~~be obtained~~determined.

Compared with the methods or models mentioned above, the advantages of the isotope matrix method include (1) the potential biases caused by multiple ~~-~~flows were taken into consideration ~~considered under~~subject to the ~~circumstance of~~constraint that there be a mass balance at the system ~~scale~~level; (2) one tracer addition was sufficient to quantify ~~for~~ multiple *in situ* flows; ~~(~~parallel incubations, i.e., ~~dark~~ light and ~~light~~ dark or $^{15}NH_4^+$ and $^{15}NO_x^-$, were not needed~~)~~; (3) ~~simple~~ post-hoc data processing was

simple, and a unique solution can be obtained via matrix ~~derivation~~inversion; (4) no extra laboratory work ~~is~~ was ~~demanded~~ necessary (see below).

4.1.2 Rate comparisons

~~Following~~ In accord with Pfister et al. (2016), we estimated all N transformation rates ~~via~~ using ordinary differential equations (ODEs) for the three cases on the assumption that ~~there is no~~ r_{NH4+}~~remineralization for comparison~~was constant (see Table 1−3). In general, the rates ~~values~~ obtained by ~~the~~ matrix inversion and integration of the ODEs were consistent. ~~The rate d~~Differences, ~~if any~~when apparent, ~~was~~ were caused by the duration ~~for~~ of the integration.~~,~~ The isotope matrix method was applied to only ~~i.e., shorter time (~~the first two time points (i.e., time intervals of either 2 or 4 hours), whereas the ODEs were integrated ~~for calculation) for isotope matrix method and longer time (4 or 5 points~~ for the entire 24-h incubation~~) for ODE~~. In Pfister et al. (2016), ODEs were used to analyze data collected at 3 ~~monitoring~~ time points within a 5-h time interval~~ours were implemented for ODE~~. Unfortunately, such intensive sampling for on-deck incubations is not practical~~; .~~ ~~however~~However, we ~~still~~ strongly recommend ~~the~~ short-term incubations for water column ~~study~~ studies~~as previously suggested~~. ~~With proper duration, t~~Two time points separated by a few hours ~~for integration~~ may be more convenient and realistic for instantaneous rate ~~measure~~estimates.

Below, we present a comparison ~~with~~ between our results and conventional source-product rate measurements (Collos, 1987) of ammonium oxidation and uptake

598 (Table 3). The matrix-derived NH_4^+ uptake rates for all of the ~~experimental~~
599 experiments ~~cases~~ were consistent with ~~those~~ the rates (difference < 8%) from the
600 traditional source-product method when the final PN concentration was ~~applied~~
601 ~~for~~used in the calculation. The fact that the deviations were larger (13−21%) when the
602 initial PN was ~~applied~~used~~, which was supported~~is consistent ~~by~~ with the conclusions
603 of previous studies that estimates involving the final PN concentration are more
604 reliable. ~~Obviously,~~The deviation could obviously be higher ~~when~~ if the
605 phytoplankton growth rate was higher.

606 ~~On the other hand~~In contrast, the end-products of ammonium oxidation or
607 nitrification are consumed by phytoplankton continuously~~, particularly~~ in the euphotic
608 ~~layer~~ zone~~full of photosynthetic autotrophs~~. In many cases, nitrate uptake has been
609 shown to occur~~s~~ in both the light and dark ~~conditions~~ (e.g. Dugdale and Goering, 1967;
610 Lipschultz, 2002; Mulholland and Lomas, 2008). The significant consumption of
611 end-products (NO_x^- and NO_2^-) ~~apparently~~ violates the ~~underlying~~ assumption ~~of~~ that
612 underlies the source-product rate calculation. Therefore, the NH_4^+
613 oxidation/nitrification rate ~~could~~ cannot ~~not~~ be ~~obtained~~determined with a
614 source-product model~~,~~. Although ~~such as all cases in our study since pp~~hytoplankton
615 consumption resulted in a net reduction of NO_x^- in all of our experiments, we were
616 nevertheless able to determine NH_4^+ oxidation/nitrification rates with the isotope
617 matrix method (Figs. 2b, 3b, and 3c) (see Table 3).

In most ~~cases~~previous studies, the final isotopic composition ~~rather than~~but not the final concentration of NO_x^- ~~was~~ has been measured~~; . as such~~As a result, researchers may not have been aware that the outflow of ~~the greater~~ $^{15}NO_x^-$ ~~outflow~~ was greater than the inflow. ~~For~~ During dark incubations, researchers may also assume insignificant NO_x^- consumption. However, ~~the~~ a "net decrease in end-product" is almost unavoidable when an incubation is conducted under simulated *in situ* light conditions ~~for~~ to estimate ammonium oxidation. To ~~overcome~~ address this consumption effect ~~induced by the first-order reaction~~, Santoro et al. (2010, 2013) took NO_x^- removal into account and formulated a new equation~~, a function of~~that took account of the nitrification rate (F) and NO_x^- uptake rate (k). ~~Following~~ In accord with Santoro et al. (2010), we calculated the nitrification rate for the low-nutrient case ~~(~~via a nonlinear least-squares curve-fitting routine in Matlab by using the first three time points of the $^{15}N\text{-}NO_x^-$ /$^{14}N\text{-}NO_x^-$ measurements~~.) to be~~The calculated rate, ~~–~~0.05 nmol L^{-1} h^{-1} (Table 3), ~~which~~ was ~~(~~~30%~~)~~ lower than the matrix-derived rate of ~~(~~0.07 nmol L^{-1} h^{-1}~~)~~. ~~By~~ In contrast, the~~ir~~ nitrate uptake rate constant ($k = 0.010\ h^{-1}$) was only one-sixth of ~~that~~ the rate constant (0.059 h^{-1}) derived from the matrix method, although a comparable nitrification rate was obtained when the consumption term was taken into account.

Surprisingly, when we introduced the values of F and k ~~two parameters by using~~determined with the method of Santoro et al. (2010) into STELLA to generate ~~the~~ time courses of ~~parameters~~variables, we found that the ~~simulations~~ simulated values of

639 $\delta^{15}NO_x^-$ and r_{NOx-} agreed well with ~~that~~ those determined ~~of~~ by the isotope matrix
640 method (Figs. 4j and 4n)~~.~~, ~~yet~~However, much slower decreasing trends were found for
641 $^{15}NO_x^-$, $^{14}NO_x^-$, and NO_x^- (Figs. 4 b, f and r)~~. —~~. Finally, we realized that the ~~formula~~
642 equation ~~produced~~ proposed by Santoro et al. (2010) ~~is~~ was constrained only by the
643 ~~ratio~~ changes of the ratios rather than by the changes of the individual concentrations
644 ~~changes in~~of $^{15}NO_x^-$ and $^{14}NO_x^-$. Thus, ~~the~~ nonlinear curve-fitting ~~method by Matlab~~
645 may ~~only~~ provide a correct simulation ~~for~~ only of the ~~ratio~~ change of the ratio. This
646 conclusion implies that the nitrate uptake rate derived from ~~the~~ non-linear curve-fitting
647 ~~method in Matlab~~ should be validated ~~also~~ by the final concentration of nitrate, as was
648 done by Santoro et al. (2013).

649 In summary, (1) ~~an~~ accurate measurements of concentrations during a time series
650 is vital for all kinds of transformation rate estimates, including the isotope matrix
651 method and (2) the isotope matrix method can ~~overcame~~ overcome various biases that
652 impact estimates made with traditional methods ~~might encounter~~.

653 **4.2 Implications for nitrogen biogeochemical processes**

654 ~~Through~~ Results of use of the isotope matrix method suggest several conclusions
655 with respect to~~,~~ biogeochemical ~~implications were obtained from various~~
656 ~~aspects~~processes.

657 **4.2.1 Remineralization, regeneration, and community succession**

The matrix solution ~~fit well~~was consistent with the model runs with variable r-NH_4^+ ~~in~~ at time points of no more than 12 h~~early stage~~, the implication being ~~suggesting~~ that dilution effects ~~was~~ were negligible during the early incubation period, at least in our ~~case~~studies. Dilution effects could be significant when remineralization is intensive and the incubation ~~prolongs~~longer. Pfister et al. (2016) found that macrofauna (mussels) play an important role in remineralization. ~~While~~ The fact that zooplankton in ~~the water column of~~ our ~~sampled cases was~~water samples were not abundant~~, it~~ might be a reason for the low remineralization rates in our short-term incubations.

In the WNP low~~-~~nutrient case, after ~~24 hour~~an incubation of 24 hours, the levels of nitrate and ammonium approached the concentration threshold for phytoplankton utilization (e.g., <30−40 nM NH_4^+ for *Emiliania huxleyi*; Sunda and Ransom, 2007). In Figure 4, the STELLA projection ~~fitted~~ agreed well with the PN ~~parameters~~ concentrations ~~only~~ for only the first 12 hours. In this case, ~~in fact,~~ we ~~have~~ actually observed phytoplankton succession. Our flow cytometry data ~~(shown in authors reply for Reviewer #2)~~(Fig. S3) ~~demonstrated~~ that the ~~cell~~ number of living ~~eukaryotes~~ eukaryotic cells (4 times higher than *Synechococcus*) increased in the first 24 hours and started to drop rapidly after 24 hours. ~~On the contrary~~In contrast, the growth of *Synechococcus* continued ~~for throughout 94~~after 24 hours, even though ~~under constantly low~~ nitrogen ~~nutrient situation~~concentrations dropped to constantly low level. ~~Such~~ These observations ~~phenomenon~~ suggest~~ed~~ that the phytoplankton

community was ~~competed~~ competing for nitrogen, ~~source~~ and a major community shift started at around 24 hours. After the time point ~~of~~ at 12 hours, the observed ~~parameters associated with~~concentrations of ^{14}N and ^{15}N in the PN ~~was~~ were higher than ~~the~~ those ~~projection~~ projected by STELLA. The most intriguing phenomenon among PN-associated parameters was the additional ^{15}N, which ~~should~~ could not have come from $^{15}NH_4^+$~~, in PN~~. The most likely source of nitrogen ~~source candidate~~ with enriched ^{15}N to support *Synechococcus* growth was the nitrogen released from dead eukaryotes, which contained freshly consumed ^{15}N tracer, rather than the ambient DON. More studies are needed to explore nutrient thresholds for different phytoplankton species. Nevertheless, our results suggest~~ed~~ that ~~short term~~ incubations ~~is crucial~~must last no more than a few hours for nitrogen uptake studies in the oligotrophic ocean.

4.2.2 ~~Evaluate~~ Evaluation of the contribution of nitrification to new production

Nitrification in the ~~sunlit~~ euphotic zone of the ocean drew ~~not much~~little attention until recent ~~decades~~ years after molecular evidence led to the discovery of the widespread occurrence of ammonia oxidizing archaea (AOA) ~~discovery in the perspective of molecular evidence~~ (Francis et al., 2005; Santoro et al., 2010, 2013; Smith et al., 2014) and rate measurements based on ~~isotope~~ isotopic studies (Ward, 2011; Santoro et al., 2010; Grundle et al., 2013; Smith et al., 2014). As mentioned in ~~Introduction~~the Introduction, the conventional "new" production ~~has~~ may have been overestimated 19−33% on a global scale due to the ~~"regenerated"~~ nitrate regenerated in

the euphotic zone via nitrification ~~process~~. However, a more realistic ~~evaluation~~ assessment of ~~for~~ the fractional contribution of nitrification to NO_3^- uptake can only be achieved when ~~the~~ incubations ~~is~~ are conducted in the same bottle under *in situ* light conditions instead of parallel incubations in the dark and light. The isotope matrix method is so far the most convenient and suitable method for evaluating the relative importance of co-occurring nitrification and new production in the euphotic ~~ocean~~zone. In all our experimental ~~cases~~studies, the contributions of nitrification to new production were < 1% (Table 4). ~~The~~ This relatively low contribution was probably due to ~~the~~ light inhibition ~~on~~ of nitrifiers ~~for~~ in the WNP ~~case~~ and ~~because of~~ the low water temperature ~~in the sampling season~~.

Nevertheless, light effects in our ~~case~~ studies ~~is~~ were significant. Light suppresses nitrification (Ward, 2005; Merbt et al., 2012; Peng et al., 2016). The NH_4^+ oxidation rate ~~in~~ at 80% sPAR was reduced by 36% relative to ~~that in~~the rate at 2% sPAR. These ~~Results~~ results ~~agreed~~ are consistent with current knowledge, although some recent evidence~~s~~ has ~~showed~~ shown that some taxa of marine AOA ~~hold~~ have the genetic ~~capabilities~~ capability to reduce oxidative stress and to repair ultraviolet damage (Luo et al., 2014; Santoro et al., 2015). More ~~study~~ case studies~~s~~ are needed in the future to explore the vertical distribution~~s~~ of the relative contribution of nitrification to new production in the euphotic zone.

4.2.3 Nutrient preference

Phytoplankton ~~takes different~~use a variety of nitrogenous species ~~as nutrients~~ for growth. McCarthy et al. (1977) introduced ~~a~~ the concept of a relative preference index (~~PRI~~RPI) to assess the relative ~~utilization~~ use of ~~a specific~~different ~~N~~ forms of N, and ~~when~~ an RPI ~~value~~ >1 indicates a preference for the specific substrate over ~~the~~ other ~~N~~ forms of N. As shown in Table 4, in the ~~NO_3^- prevailed~~ low nutrient case NO_3^- was preferred~~,~~. ~~the~~ The fact that the ~~PRI~~ RPI for ~~(~~NO_3^-~~)~~ was ~~very close but~~ slightly higher ~~to~~ ~~PRI~~than the RPI for ~~(~~NH_4^+~~),~~ ~~which~~ was probably due to the phytoplankton community structure, as mentioned above. This result ~~was in line~~is consistent with ~~the results~~studies in the Sargasso Sea (Fawcett et al., 2011). ~~While~~ However, in the high-nutrient case ~~NH_4^+ bay~~, the order of the RPI values was ~~PRI (~~NH_4^+ ~~)~~ > 1 > ~~PRI (~~NO_3^-~~)~~ > ~~PRI (~~NO_2^-~~)~~, the ~~suggesting~~ suggestion being that phytoplankton preferred NH_4^+ over NO_3^- and NO_2^-, similar to the ~~the~~ results of studies in Chesapeake Bay (McCarthy et al., 1977).

4.2.4 Quantifying various ammonium consumption pathways

In the upper ocean, NH_4^+ cycles rapidly due to the metabolic pathways of the various microorganisms~~'s~~ that ~~metabolic pathways~~ competeing for ammonium. Ammonium may serve as a nitrogen source for phytoplankton assimilation, and as an energy source for ammonia-~~-~~oxidizing organisms (AOM). Moreover, many studies have shown that bacteria also play a part in NH_4^+ utilization (Middelburg and Nieuwenhuize, 2000; Veuger et al., 2004). Our results in the low-~~-~~nutrient case showed that phytoplankton ~~was~~ were the main consumers of NH_4^+ ~~consumer~~ (82% of the total NH_4^+ consumption~~),~~). ~~bacteria~~ Bacteria accounted for another ~17%, and AOM

~~utilized~~ used the ~~rest~~ remaining 1%. ~~While i~~In the high-nutrient study~~eutrophic WYW bay~~, phytoplankton and bacteria each consumed ~50% of the total NH_4^+ (Table 4).

5. Conclusions

The~~is~~ isotope matrix method was designed specifically for ~~euphotic water column~~ incubations in the euphotic zone under simulated *in situ* conditions. By considering multiple ~~-~~flows among pools ~~on the assumption of~~and requiring mass balance at the whole~~-~~-system level, we minimized potential biases caused by non-targeted processes in traditional source-product methods. Given the progress in analytical techniques for measuring concentrations and isotopic compositions of nitrogen species, the isotope matrix method ~~presents~~ is a promising ~~avenue~~ approach for ~~the~~ studying of rates of nitrogen ~~processes~~ fluxes ~~with~~ from a system-wide perspective. Furthermore, the matrix method is also appropriate for probing the effects of environmental factors (e.g., CO_2, pH, temperature, and light intensity) on ~~the~~ interactive N processes in ~~one~~ a single incubation bottle.

Acknowledgement

We sincerely thank Wenbin Zou and Tao Huang at the State Key Laboratory of Marine Environmental Science (Xiamen University, China) for their valuable help with the water sampling and the on-board trace NH_4^+ concentration analysis during the 2015 NWP cruise. Yu-ting Shih from the Department of Geology at National Taiwan University in Taiwan is thanked for his help on ODE application. This research was

761 funded by the National Natural Science Foundation of China (NSFC U1305233,
762 2014CB953702, 91328207, 2015CB954003).

763 **References**

764 Beman, J. M., Popp, B. N., and Alford, S. E.: Quantification of ammonia oxidation
765 rates and ammonia-oxidizing archaea and bacteria at high resolution in the Gulf of
766 California and eastern tropical North Pacific Ocean, Limnol. Oceanogr., 57, 711-726,
767 doi: 10.4319/lo.2012.57.3.0711, 2012.

768 Blackburn, T. H.: Method for Measuring Rates of NH_4^+ Turnover in Anoxic Marine
769 Sediments, Using a ^{15}N-NH_4^+ Dilution Technique, Appl. Environ. Microbiol., 37,
770 760-765, 1979.

771 Braman, R. S., and Hendrix, S. A.: Nanogram nitrite and nitrate determination in
772 environmental and biological materials by vanadium (III) reduction with
773 chemiluminescence detection, Anal. Chem., 61, 2715-2718, doi: 10.1021/ac00199a007,
774 1989.

775 Brauwere, A. D., Ridder, F. D., Pintelon, R., Elskens, M., Schoukens, J., and Baeyens,
776 W.: Model selection through a statistical analysis of the minimum of a weighted least
777 squares cost function, Chemom. Intell. Lab. Syst., 76, 163-173, doi:
778 10.1016/j.chemolab.2004.10.006, 2005.

779 Bronk, D., Killberg-Thoreson, L., Sipler, R., Mulholland, M., Roberts, Q., Bernhardt,
780 P., Garrett, M., O'Neil, J., and Heil, C.: Nitrogen uptake and regeneration (ammonium
781 regeneration, nitrification and photoproduction) in waters of the West Florida Shelf
782 prone to blooms of Karenia brevis, Harmful Algae, 38, 50-62, doi:
783 10.1016/j.hal.2014.04.007, 2014.

784 Bronk, D. A., and Glibert, P. M.: A ^{15}N tracer method for the measurement of dissolved
785 organic nitrogen release by phytoplankton, Mar. Ecol. Prog. Ser., Marine Ecology
786 Progress, 77, 1991.

787 Bronk, D, A, and Glibert, P, M.: The fate of the missing ^{15}N differs among marine
788 systems, Limnol. and Oceanogr., 39(1), 189-195, doi: 10.4319/lo.1994.39.1.0189
789 1994.

790 Bronk, D. A., Glibert, P. M., and Ward, B. B.: Nitrogen uptake, dissolved organic
791 nitrogen release, and new production, Science, 265, 1843-1846, 1994.

Bronk, D. A., and Ward, B. B.: Magnitude of dissolved organic nitrogen release relative to gross nitrogen uptake in marine systems, Limnol. Oceanogr., 45, 1879-1883, doi: 10.4319/lo.2000.45.8.1879, 2000.

Caperon, J., Schell, D., Hirota, J., and Laws, E.: Ammonium excretion rates in Kaneohe Bay, Hawaii, measured by a ^{15}N isotope dilution technique, Mar. Biol., 54, 33-40, doi: 10.1007/BF00387049, 1979.

Casciotti, K., Sigman, D., Hastings, M. G., Böhlke, J., and Hilkert, A.: Measurement of the oxygen isotopic composition of nitrate in seawater and freshwater using the denitrifier method, Anal. Chem., 74, 4905-4912, 2002.

Casciotti, K. L.: Nitrogen and Oxygen Isotopic Studies of the Marine Nitrogen Cycle, Ann. Rev. Mar. Sci., 8, 379-407, doi: 10.1146/annurev-marine-010213-135052, 2016.

Chen, Y.-l. L.: Spatial and seasonal variations of nitrate-based new production and primary production in the South China Sea, Deep Sea Res. Part I Oceanogr. Res. Pap., 52, 319-340, doi: 10.1016/j.dsr.2004.11.001, 2005.

Collos, Y.: Calculations of ^{15}N uptake rates by phytoplankton assimilating one or several nitrogen sources, International Journal of Radiation Applications and Instrumentation. Part A. Applied Radiation and Isotopes, 38, 275-282, doi: 10.1016/0883-2889(87)90038-4, 1987.

Coplen, T. B, Krouse, H. R, and Böhlke, J. K.: Reporting of nitrogen isotope abundances-(Technical report). Pure and Applied Chemistry, 907-908, 1992.

Daims, H., Lebedeva, E. V., Pjevac, P., Han, P., Herbold, C., Albertsen, M., Jehmlich, N., Palatinszky, M., Vierheilig, J., Bulaev, A., Kirkegaard, R. H., von Bergen, M., Rattei, T., Bendinger, B., Nielsen, P. H., and Wagner, M.: Complete nitrification by Nitrospira bacteria, Nature, 528, 504-509, 10.1038/nature16461, doi: 10.1038/nature16461, 2015.

Dore, J. E., and Karl, D. M.: Nitrification in the euphotic zone as a source for nitrite, nitrate, and nitrous oxide at Station ALOHA, Limnol. Oceanogr., 41(8):1619-1628, 1996.

Dugdale, R., and Goering, J.: Uptake of new and regenerated forms of nitrogen in primary productivity, Limnol. Oceanogr., 12, 196-206, doi: 10.4319/lo.1967.12.2.0196, 1967.

Dugdale, R., and Wilkerson, F.: The use of ^{15}N to measure nitrogen uptake in eutrophic oceans; experimental considerations, Limnol. Oceanogr., 31, 673-689, doi: 10.4319/lo.1986.31.4.0673, 1986.

Elskens, M., Baeyens, W., Cattaldo, T., Dehairs, F., and Griffiths, B.: N uptake conditions during summer in the Subantarctic and Polar Frontal Zones of the Australian

828 sector of the Southern Ocean, J. Geophys. Res.: Oceans, 107, 3-1-3-11, doi:
829 10.1029/2001JC000897, 2002.

830 Elskens, M., Baeyens, W., Brion, N., Galan, S. D., Goeyens, L., and Brauwere, A. D.:
831 Reliability of N flux rates estimated from ^{15}N enrichment and dilution experiments in
832 aquatic systems, Global Biogeochem. Cycles, 19, 573-574, doi:
833 10.1029/2004GB002332, 2005.

834 Falkowski, P. G.: Evolution of the nitrogen cycle and its influence on the biological
835 sequestration of CO_2 in the ocean, Nature, 387, 272-275, doi: 10.1038/387272a0, 1997.

836 Fawcett, S. E., Lomas, M. W., Casey, J. R., Ward, B. B., and Sigman, D. M.:
837 Assimilation of upwelled nitrate by small eukaryotes in the Sargasso Sea, Nature
838 Geoscience, 4, 717-722, doi: 10.1038/ngeo1265, 2011.

839 Francis, C. A., Roberts, K. J., Beman, J. M., Santoro, A. E., and Oakley, B. B.: Ubiquity
840 and diversity of ammonia-oxidizing archaea in water columns and sediments of the
841 ocean, Proceedings of the National Academy of Sciences, 102, 14683-14688, doi:
842 10.1073/pnas.0506625102, 2005.

843 Gilbert, P. M., Lipschultz, F., McCarthy, J. J., and Altabet, M. A.: Isotope dilution
844 models of uptake and remineralization of ammonium by marine plankton, Limnol.
845 Oceanogr., 27, 639-650, 1982.

846 Granger, J., and Sigman, D. M.: Removal of nitrite with sulfamic acid for nitrate N and
847 O isotope analysis with the denitrifier method, Rapid Commun. Mass Spectrom., 23,
848 3753-3762, 10.1002/rcm.4307, doi: 10.1002/rcm.4307, 2009.

849 Grundle, D. S., Juniper, S. K., and Giesbrecht, K. E.: Euphotic zone nitrification in the
850 NE subarctic Pacific: Implications for measurements of new production, Mar. Chem.,
851 155, 113-123, doi: 10.1016/j.marchem.2013.06.004, 2013.

852 Hannon, J. E., and Böhlke, J. K.: Determination of the delta ($^{15}N/^{14}N$) of Ammonium
853 (NH_4^+) in Water: RSIL Lab Code 2898, US Geological Survey 2328-7055, 2008.

854 Harrison, P. J., and Davis, C. O.: Use of the perturbation technique to measure nutrient
855 uptake rates of natural phytoplankton populations, Deep Sea Res., 24, 247-255, doi:
856 10.1016/S0146-6291(77)80003-9, 1977.

857 Harrison, W. G., Harris, L. R., Karl, D. M., Knauer, G. A., and Redalje, D.G.: Nitrogen
858 dynamics at the VERTEX time-series site, Deep Sea Res. Part I Oceanogr. Res. Pap.,
859 39(9):1535-1552, doi: 10.1016/0198-0149(92)90046-V, 1992.

860 Harvey, W. A., and Caperon, J.: The rate of utilization of urea, ammonium, and nitrate
861 by natural populations of marine phytoplankton in a eutrophic environment, Pacific
862 Science, 30 (4), 329-340, http://hdl.handle.net/10125/1169, 1976.

Holmes, R., McClelland, J., Sigman, D., Fry, B., and Peterson, B.: Measuring ^{15}N–NH_4^+ in marine, estuarine and fresh waters: An adaptation of the ammonia diffusion method for samples with low ammonium concentrations, Mar. Chem., 60, 235-243, doi: 10.1016/S0304-4203(97)00099-6, 1998.

Horrigan, S., Carlucci, A., and Williams, P.: Light inhibition of nitrification in sea-surface films [California], J. Mar. Res., 1981.

Howard, M. D. A., Cochlan, W. P., Ladizinsky, N., and Kudela, R. M.: Nitrogenous preference of toxigenic Pseudo-nitzschia australis (Bacillariophyceae) from field and laboratory experiments, Harmful Algae, 6, 206-217, doi: 10.1016/j.hal.2006.06.003, 2007.

Hsiao, S.-Y., Hsu, T.-C., Liu, J.-w., Xie, X., Zhang, Y., Lin, J., Wang, H., Yang, J.-Y., Hsu, S.-C., and Dai, M.: Nitrification and its oxygen consumption along the turbid Chang Jiang River plume, Biogeosciences, 11, 2083-2098, doi: 10.5194/bg-11-2083-2014, 2014.

Knapp, A. N., Sigman, D. M., and Lipschultz, F.: N isotopic composition of dissolved organic nitrogen and nitrate at the Bermuda Atlantic Time-series Study site, Global Biogeochem. Cycles, 19, doi: 10.1029/2004GB002320, 2005.

Koroleff, F.: Simultaneous oxidation of nitrogen and phosphorus compounds by persulfate, Methods of seawater analysis, 2, 205-206, 1983.

Laws, E, A., and Wong, D. C. L.: Studies of carbon and nitrogen metabolism by three marine phytoplankton species in nitrate−limited continuous culture, Journal of Phycology, 14(4): 406-416, doi: 10.1111/j.1529-8817.1978.tb02460.x, 1978.

Laws, E. A.: Analytic Models of NH_4^+ Uptake and Regeneration Experiments, Limnol. Oceanogr., 30, 1340–1350, doi: 10.4319/lo.1985.30.6.1340, 1985.

Laws, E. A., Landry, M. R., Barber, R, T., Lisa Campbellc, Mary-Lynn Dicksond, and John Marra.: Carbon cycling in primary production bottle incubations: inferences from grazing experiments and photosynthetic studies using ^{14}C and ^{18}O in the Arabian Sea, Deep Sea Res. Part II Top. Stud. Oceanogr., 47(7): 1339-1352, doi: 10.1016/S0967-0645(99)00146-0, 2000.

Lipschultz, F.: A time-series assessment of the nitrogen cycle at BATS, Deep Sea Res. Part II Top. Stud. Oceanogr., 48, 1897-1924, doi: 10.1016/S0967-0645(00)00168-5, 2001.

Lipschultz, F.: Isotope Tracer Methods for Studies of the Marine Nitrogen Cycle, in Nitrogen in the marine environment, edited by: Capone, D. A., Bronk, D. A., Mulholland, M. R., Carpenter, E. J., Academic Press, London, U.K., 303-384, 2008.

Lomas, M. W., and Lipschultz, F.: Forming the primary nitrite maximum: Nitrifiers or phytoplankton?, Limnol. Oceanogr., 51, 2453-2467, doi: 10.4319/lo.2006.51.5.2453, 2006.

Luo, H., Tolar, B. B., Swan, B. K., Zhang, C. L., Stepanauskas, R., Ann, M. M., and Hollibaugh, J. T.: Single-cell genomics shedding light on marine Thaumarchaeota diversification, ISME Journal, 8, 732-736, doi: 10.1038/ismej.2013.202, 2014.

Marchant, H. K., Mohr, W., Kuypers, M. M. M.: Recent advances in marine N-cycle studies using ^{15}N labeling methods. Curr. Opin. Biotechnol., 41, 53-59, doi: 10.1016/j.copbio.2016.04.019, 2016.

McCarthy, J. J., and Eppley, R. W.: A comparison of chemical, isotopic, and enzymatic methods for measuring nitrogen assimilation of marine phytoplankton, Limnol. Oceanogr., 17, 371-382, doi: 10.4319/lo.1972.17.3.0371, 1972.

Mccarthy, J. J., Taylor, and Taft, J. L.: Nitrogenous nutrition of the plankton in the Chesapeake Bay.1. Nutrient availability and phytoplankton preferences, Limnol. Oceanogr., 22, 996-1011, 1977.

McIlvin, M. R., and Altabet, M. A.: Chemical conversion of nitrate and nitrite to nitrous oxide for nitrogen and oxygen isotopic analysis in freshwater and seawater, Anal. Chem., 77, 5589-5595, doi: 10.1021/ac050528s, 2005.

Merbt, S. N., Stahl, D. A., Casamayor, E. O., Mart ́ı, E., Nicol, G. W., and Prosser, J. I.: Differential photoinhibition of bacterial and archaeal ammonia oxidation, FEMS Microbiol. Lett., 327, 41-46, doi: http://dx.doi.org/10.1111/j.1574-6968.2011.02457.x, 2012.

Middelburg, J. J., and Nieuwenhuize, J.: Uptake of dissolved inorganic nitrogen in turbid, tidal estuaries, Mar. Ecol. Prog. Ser., 192, 79-88, doi: 10.3354/meps192079, 2000.

Mulholland, M. R., and Lomas, M. W.: Nitrogen uptake and assimilation, in Nitrogen in the marine environment, edited by: Capone, D. A., Bronk, D. A., Mulholland, M. R., Carpenter, E. J., Academic Press, London, U.K., 303-384, 2008.

Newell, S. E., Fawcett, S. E., and Ward, B. B.: Depth distribution of ammonia oxidation rates and ammonia-oxidizer community composition in the Sargasso Sea, Limnol. Oceanogr., 58, 1491-1500, doi: 10.4319/lo.2013.58.4.1491, 2013.

Olson, R.: ^{15}N tracer studies of the primary nitrite maximum, J. Mar. Res., 39, 203-226, 1981a.

Olson, R. J.: Differential photoinhibition of marine nitrifying bacteria: a possible mechanism for the formation of the primary nitrite maximum, J. Mar. Res., 39, 227-238, 1981b.

934 Painter, S. C., Patey, M. D., Tarran, G. A., and Torres-Valdés, S.: Picoeukaryote
935 distribution in relation to nitrate uptake in the oceanic nitracline, Aquat. Microb. Ecol.,
936 72, 195-213, doi: 10.3354/ame01695, 2014.

937 Pakulski, J., Benner, R., Amon, R., Eadie, B., and Whitledge, T.: Community
938 metabolism and nutrient cycling in the Mississippi River plume: evidence for intense
939 nitrification at intermediate salinities, Mar. Ecol. Prog. Ser., 117, 207, 1995.

940 Peng, X., Fuchsman, C. A., Jayakumar, A., Warner, M. J., Devol, A. H., and Ward, B.
941 B.: Revisiting nitrification in the eastern tropical South Pacific: A focus on controls, J.
942 Geophys. Res.: Oceans, doi: 10.1002/2015JC011455, 2016.

943 Pfister, C. A., Altabet, M. A., Pather, S., and Dwyer, G.: Tracer experiment and model
944 evidence for macrofaunal shaping of microbial nitrogen functions along rocky shores,
945 Biogeosciences, 13, 3519-3531, doi: 10.5194/bg-13-3519-2016, 2016.

946 Raimbault, P., and Garcia, N.: Evidence for efficient regenerated production and
947 dinitrogen fixation in nitrogen-deficient waters of the South Pacific Ocean: impact on
948 new and export production estimates, Biogeosciences, 5, 323-338, 2008.

949 Santoro, A., Sakamoto, C., Smith, J., Plant, J., Gehman, A., Worden, A., Johnson, K.,
950 Francis, C., and Casciotti, K.: Measurements of nitrite production in and around the
951 primary nitrite maximum in the central California Current, Biogeosciences, 10,
952 7395-7410, doi: 10.5194/bg-10-7395-2013, 2013.

953 Santoro, A. E., Casciotti, K. L., and Francis, C. A.: Activity, abundance and diversity of
954 nitrifying archaea and bacteria in the central California Current, Environ. Microbiol.,
955 12, 1989-2006, doi. L., and Francis, C. A.: Activity, abundance and diversity of
956 nitrifying archaea and bacteria in the central California Current, Environ. Microbiol.,
957 12, 1989-2006, 2010.

958 Santoro, A. E., Dupont, C. L., Richter, R. A., Craig, M. T., Carini, P., Mcilvin, M. R.,
959 Yang, Y., Orsi, W. D., Moran, D. M., and Saito, M. A.: Genomic and proteomic
960 characterization of "Candidatus Nitrosopelagicus brevis": An ammonia-oxidizing
961 archaeon from the open ocean, Proceedings of the National Academy of Sciences of the
962 United States of America, 112, 1173-1178, doi: 10.1073/pnas.1416223112, 2015.

963 Sigman, D., Casciotti, K., Andreani, M., Barford, C., Galanter, M., and Böhlke, J.: A
964 bacterial method for the nitrogen isotopic analysis of nitrate in seawater and freshwater,
965 Anal. Chem., 73, 4145-4153, doi: 10.1021/ac010088e, 2001.

966 Smith, J. M., Chavez, F. P., and Francis, C. A.: Ammonium uptake by phytoplankton
967 regulates nitrification in the sunlit ocean, PloS One, 9, e108173, doi:
968 org/10.1371/journal.pone.0108173, 2014.

969 Sunda, W. G., and Ransom, H. D.: Ammonium uptake and growth limitation in marine
970 phytoplankton, Limnol. Oceanogr., 52, 2496–2506, 2007.

971 van Kessel, M. A., Speth, D. R., Albertsen, M., Nielsen, P. H., Opden Camp, H. J.,
972 Kartal, B., Jetten, M. S., and Lucker, S.: Complete nitrification by a single
973 microorganism, Nature, 528, 555-559, 10.1038/nature16459, doi:
974 10.1038/nature16459, 2015.

975 Varela, M. M., Bode, A., Fernandez, E., Gonzalez, N., Kitidis, V., Varela, M., and
976 Woodward, E.: Nitrogen uptake and dissolved organic nitrogen release in planktonic
977 communities characterised by phytoplankton size–structure in the Central Atlantic
978 Ocean, Deep Sea Res. Part I Oceanogr. Res. Pap., 52, 1637-1661, doi:
979 10.1016/j.dsr.2005.03.005, 2005.

980 Veuger, B., Middelburg, J. J., Boschker, H. T. S., Nieuwenhuize, J., Rijswijk, P. V.,
981 Rochelle-Newall, E. J., and Navarro, N.: Microbial uptake of dissolved organic and
982 inorganic nitrogen in Randers Fjord, Estuarine Coastal and Shelf Science, 61, 507–515,
983 doi: 10.1016/j.ecss.2004.06.014, 2004.

984 Wada, E., and Hatton, A.: Nitrite metabolism in the euphotic layer of the central North
985 Pacific Ocean, Limnol. Oceanogr., 16, 766-772, doi: 10.4319/lo.1971.16.5.0766 1971.

986 Ward, B. B.: Temporal variability in nitrification rates and related biogeochemical
987 factors in Monterey Bay, California, USA, Mar. Ecol. Prog. Ser., 292, 109, doi:
988 10.3354/meps292097, 2005.

989 Ward, B. B.: Nitrification in marine systems, in Nitrogen in the marine environment,
990 edited by: Capone, D. A., Bronk, D. A., Mulholland, M. R., Carpenter, E. J., Academic
991 Press, London, U.K., 5, 199-261, 2008.

992 Ward, B. B.: Measurement and distribution of nitrification rates in the oceans, in
993 Methods in enzymology, edited by Abelson, J. N., Simon, M. I., Academic Press,
994 London, U.K., 486, 307-323, 2011.

995 Yool, A., Martin, A. P., Fernández, C., and Clark, D. R.: The significance of
996 nitrification for oceanic new production, Nature, 447, 999-1002, doi:
997 10.1038/nature05885, 2007.

998 Zehr, J. P., and Kudela, R. M.: Nitrogen cycle of the open ocean: from genes to
999 ecosystems, Ann. Rev. Mar. Sci., 3, 197-225, doi:
1000 10.1146/annurev-marine-120709-142819, 2011.

1001 Zhang, L., Altabet, M. A., Wu, T., and Hadas, O.: Sensitive measurement of NH_4^+
1002 $^{15}N/^{14}N$ ($\delta^{15}NH_4^+$) at natural abundance levels in fresh and saltwaters, Anal. Chem., 79,
1003 5297-5303, doi: 10.1021/ac070106d, 2007.

1004 Zhu, Y., Yuan, D., Huang, Y., Ma, J., and Feng, S.: A sensitive flow-batch system for
1005 on board determination of ultra-trace ammonium in seawater: Method development and
1006 shipboard application, Anal. Chim. Acta., 794, 47-54, 10.1016/j.aca.2013.08.009, doi:
1007 10.1016/j.aca.2013.08.009, 2013.

1008

Table 1. The isotope matrix results for (A) the specific rates and (B) average rates of N processes in the low-nutrient case during the first interval under different r_{NH4+} variation conditions. And all N transformation rates via ODE following Pfister et al. (2016) on the assumption of no remineralization were estimated for comparison. Note r_{NH4+} variation was manipulated artificially by decreasing r_{NH4+} values at a constant reduction rate and the total reduction of r_{NH4+} was 0%, 1%, 10%, 20% and 50% of the full time span (24 h) of incubation.

(A)

Rate constant (k) h^{-1}	The percentage of r_{NH4+} decrease in 24 h					
	0		1%	10%	20%	50%
	ODE	Isotope Matrix				
NH_4^+ uptake (k1)	0.040	0.038	0.038	0.038	0.038	0.039
Remineralization (k2)	0	0	0.00001	0.0001	0.0002	0.001
NH_4^+ oxidation (k3)	0.0004	0.0005	0.0005	0.0005	0.0005	0.0005
NO_x^- uptake (k4)	0.060	0.059	0.059	0.059	0.059	0.059
DON release (k5)	0.017	0.024	0.024	0.024	0.024	0.024
Bacteria uptake NH_4^+ (k6)	0.005	0.007	0.008	0.011	0.015	0.028

(B)

Rate ($k \times \bar{C}$) nmol L^{-1} h^{-1}	The percentage of r_{NH4+} decrease in 24 h					
	0		1%	10%	20%	50%
	ODE	Isotope Matrix				
NH_4^+ uptake (F1)	3.8	4.9	4.9	4.9	5.0	5.1
Remineralization (F2)	0.0	0.0	0.1	0.6	1.2	3.0
NH_4^+ oxidation (F3)	0.04	0.07	0.1	0.1	0.1	0.7
NO_x^- uptake (F4)	19.3	27.2	27.2	27.2	27.2	27.2
DON release (F5)	9.6	11.5	11.5	11.6	11.6	11.8
Bacteria uptake NH_4^+ (F6)	0.5	1.0	1.0	1.5	2.0	3.7

Table 2. The isotope matrix results for the rates of N processes in the high-nutrient case at the depth of (A) 80% sPAR and (B) 2% sPAR under different r_{NH4+} variation conditions. And all N transformation rates via ODE following Pfister et al. (2016) on the assumption of no remineralization were estimated for comparison. Note: r_{NH4+} variation was manipulated artificially by decreasing r_{NH4+} values at a constant reduction rate and the total reduction of r_{NH4+} was 0%, 1%, 10%, 20% and 50% of the full time span (15 h) of incubation.

(A)

Rate ($k^*\ \bar{C}$) nmol L^{-1} h^{-1}	The percentage of r_{NH4+} decrease in 15 h					
	0		1%	10%	20%	50%
	ODE	Isotope Matrix				
NH_4^+ uptake (F1)	360	397	397	399	401	408
Remineralization (F2)	0	0	21	211	424	1043
NO_2^- uptake (F3)	27	29	29	29	29	29
NH_4^+ oxidation (F4)	1.1	0.4	0.4	0.4	0.4	0.4
NO_3^- uptake (F5)	190	149	149	149	149	149
NO_2^- oxidation (F6)	1.7	0	0	0	0	0
DON release (F7)	0	0	0	0	0	0
Bacteria uptake NH_4^+ (F8)	268	282	303	490	701	1314

(B)

Rate ($k^*\ \bar{C}$) nmol L^{-1} h^{-1}	The percentage of r_{NH4+} decrease in 15 h					
	0		1%	10%	20%	50%
	ODE	Isotope Matrix				
NH_4^+ uptake (F1)	228	208	208	209	211	216
Remineralization (F2)	0	0	18.1	179	361	895
NO_2^- uptake (F3)	7.3	3.1	3.1	3.1	3.1	3.1
NH_4^+ oxidation (F4)	1.1	0.7	0.7	0.7	0.7	0.7
NO_3^- uptake (F5)	106	72	72	72	72	72
NO_2^- oxidation (F6)	2.0	0	0	0	0	0
DON release (F7)	0	0	0	0	0	0
Bacteria uptake NH_4^+ (F8)	202	265	283	442	623	1152

Table 3. Comparison of the NH_4^+/ NO_x^- uptake and NH_4^+ oxidation/nitrification rates derived from different methods.

Process	Case	Depth (m)	Isotope Matrix method (this study)	Rates based on Ref A*	Traditional method Ref B*	Rates followed Ref C*
			($nmol\ L^{-1}\ h^{-1}$)			
NH_4^+ uptake	Low nutrient	25	4.9	3.8	4.6	
Nitrification	Low nutrient	25	0.07	0.04	−	0.05
NO_x^- uptake	Low nutrient	25	27.2	19.3		4.6
NH_4^+ uptake	High -80%sPAR	0.2	397	360	387	
NH_4^+ oxidation	High -80%sPAR	0.2	0.4	1	−	
NH_4^+ uptake	High -2% sPAR	2.3	208	228	192	
NH_4^+ oxidation	High -2% sPAR	2.3	0.7	1	−	

Ref A* stands of rates calculation by ODE followed Pfister et al. (2016)

Ref B* stands of rates calculation followed Collos (1987)

Ref C* stands of rates calculation followed Santoro et al. (2010)

Table 4. The contribution of nitrification derived NO_x^- to NO_x^- uptake (%), N preference index, and the proportion of NH_4^+ consumption by phytoplankton, bacteria and nitrifier to total NH_4^+ consumption in low and high nutrient cases.

Case	Depth (m)	nitrification to NO_3^- uptake (%)	RPI for NH_4^+	RPI for NO_2^-	RPI for NO_3^-	*A/TNH_4^+ consumption (%)	*B/TNH_4^+ consumption (%)	*C/TNH_4^+ consumption (%)
Low nutrient	25	0.3	0.9		1.0	82.1	16.8	1.2
High -80%sPAR	0.2	0.3	1.6	0.6	0.5	58.4	41.5	0.1
High -2% sPAR	2.3	0.9	1.8	0.1	0.5	43.9	56.0	0.1

*A, *B, *C stands for NH_4^+ utilized by phytoplankton, bacteria and nitrifier, respectively. TNH_4^+ consumption stands for total NH_4^+ consumption.

Figure Captions

Fig. 1. Model schemes with the most fundamental nitrogen transformation processes in low- (a) and high- (b) nutrient aquatic environments. Arrows stand for the transfer flux/rate from the reactant to product pool. The structure and inter-exchanges in the high-nutrient case (Fig. 1b) are the same as in (a), except that NO_x^- is divided into NO_2^- and NO_3^-.

Fig. 2. The observational data in the low-nutrient case for (a) $[NH_4^+]$, (b) $[NO_x^-]$, (c) [PN], (d) [TDN], (e) $\delta^{15}N\text{-}NO_x^-$, (f) $\delta^{15}N\text{-}PN$. The regular and inverse open triangles stand for the paralled samples and the analytical errors are shown.

Fig. 3. The observational data in the high-nutrient case for (a) $[NH_4^+]$, (b) $[NO_2^-]$, (c) $[NO_3^-]$, (d) [PN], (e) [TDN], (f) [PN+TDN], (g) $\delta^{15}N\text{-}NO_2^-$, (h) $\delta^{15}N\text{-}NO_3^-$ and (i) $\delta^{15}N\text{-}PN$. The light and dark red diamonds stand for the paralled samples in 80% sPAR case and the black regular and inverse open triangles stand for the paralled samples in 2% sPAR case. The analytical errors are shown in figures.

Fig. 4. The observed and STELLA-derived values in the low-nutrient case for (a) $[^{15}NH_4^+]$, (b) $[^{15}NO_x^-]$, (c) [^{15}N-PN], (d) [^{15}N-DON], (e) $[^{14}NH_4^+]$, (f) $[^{14}NO_x^-]$, (g) [^{14}N-PN], (h) [^{14}N-DON], (i) r_{NH4+}, (j) r_{NOx-}, (k) r_{PN}, (l) r_{DON}, (m) $\delta^{15}N\text{-}NH_4^+$, (n) $\delta^{15}N\text{-}NO_x^-$, (o) $\delta^{15}N\text{-}PN$, (p) $\delta^{15}N\text{-}DON$, (q) $[NH_4^+]$, (r) $[NO_x^-]$, (s) [PN] and (t) [DON]. The black regular and inverse open triangles represent the paralleled observed values; the black, green, blue, magenta and pink solid lines stand for the STELLA model simulations when r_{NH4+} decreases 0%, 1%, 10%, 20% and 50% in 24 h, respectively. The dashed lines in (b), (f), (j), (n) and (r) were generated from nonlinear least-squares curve-fitting by Matlab following Santoro et al. (2010).

Fig. 5. The observed and STELLA-derived values in the high-nutrient case of (A) 80% sPAR depth and (B) 2% sPAR depth for (a) $[^{15}NH_4^+]$, (b) $[^{15}NO_2^-]$, (c) $[^{15}NO_3^-]$, (d) [^{15}N-PN], (e) [^{15}N-DON], (f) $[^{14}NH_4^+]$, (g) $[^{14}NO_2^-]$, (h) $[^{14}NO_3^-]$, (i) [^{14}N-PN], (j)

[^{14}N-DON], (k) r_{NH4+}, (l) r_{NO2-}, (m) r_{NO3-}, (n) r_{PN}, (o) r_{DON}, (p) δ^{15}N-NH_4^+, (q) δ^{15}N-NO_2^-, (r) δ^{15}N-NO_3^-, (s) δ^{15}N-PN, (t) δ^{15}N-DON, (u) [NH_4^+], (v) [NO_2^-], (w) [NO_3^-] (x) [PN] and (y) [DON]. The black regular and inverse open triangles represent the duplicate observational values; the black, green, blue, magenta and pink solid lines represent the STELLA model simulations of r_{NH4+} decreases 0%, 1%, 10%, 20% and 50% in 15 h, respectively.

1072 **Fig. 1**

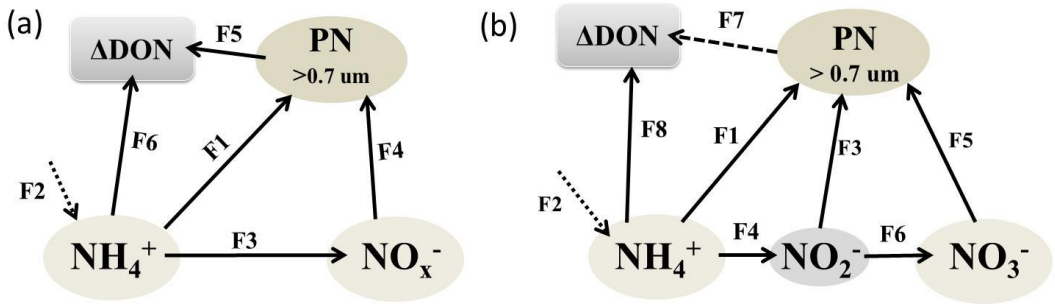

1073

1074

1075 **Fig. 2**

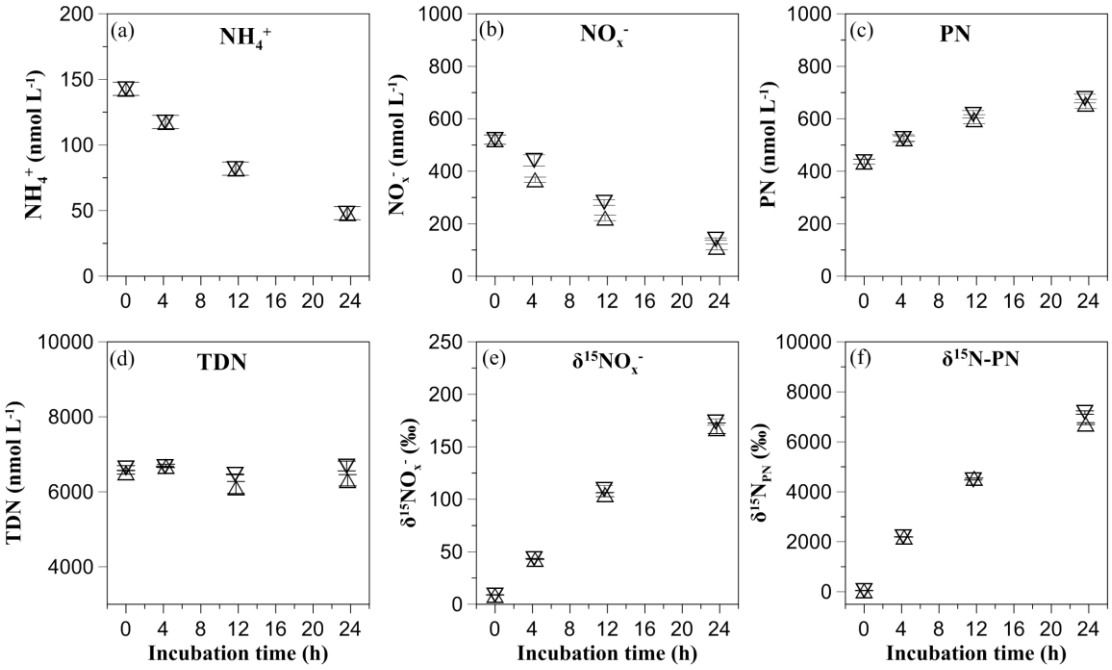

1076

1077

1078 **Fig. 3**

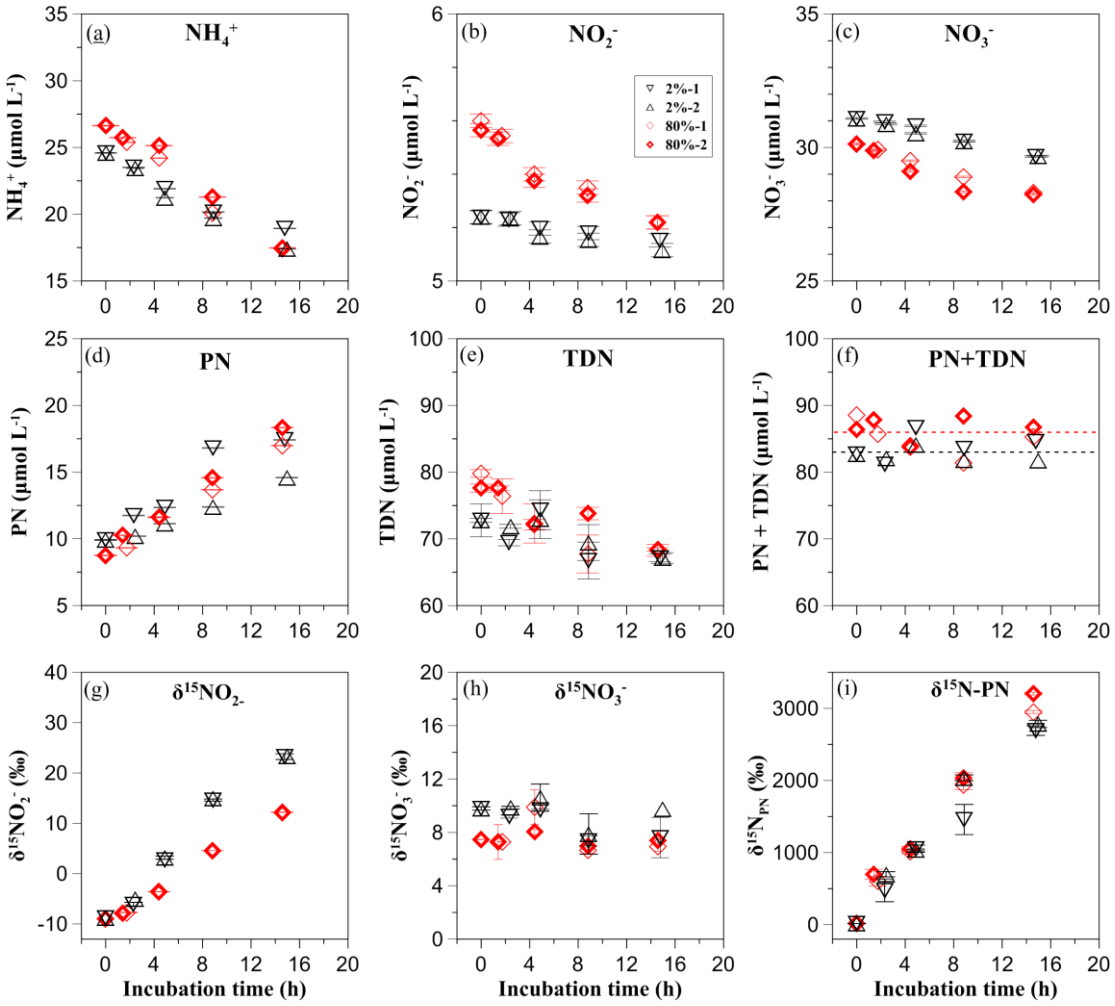

1079

1080

1081 **Fig. 4**

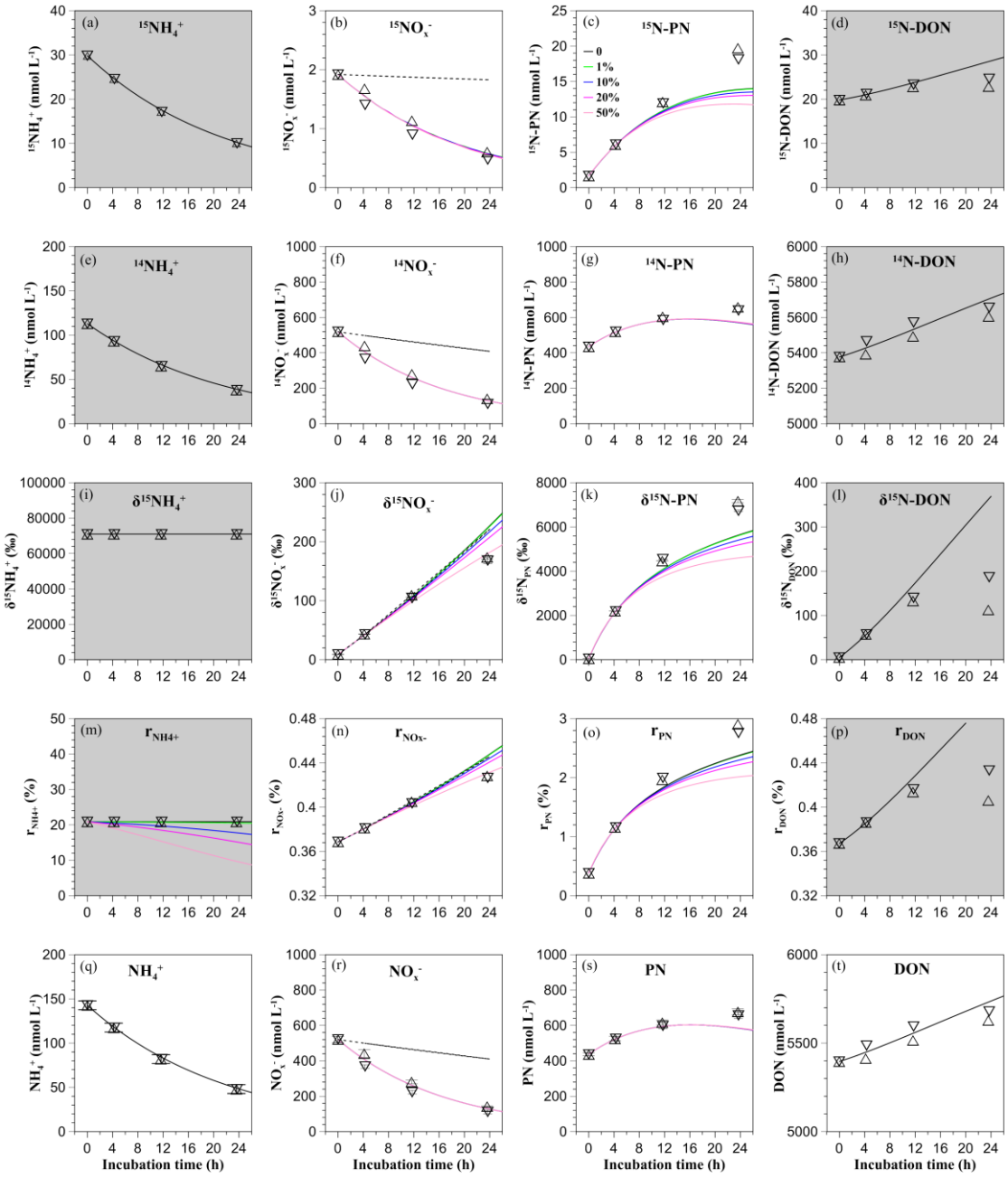

1082

1083

Fig. 5(A)

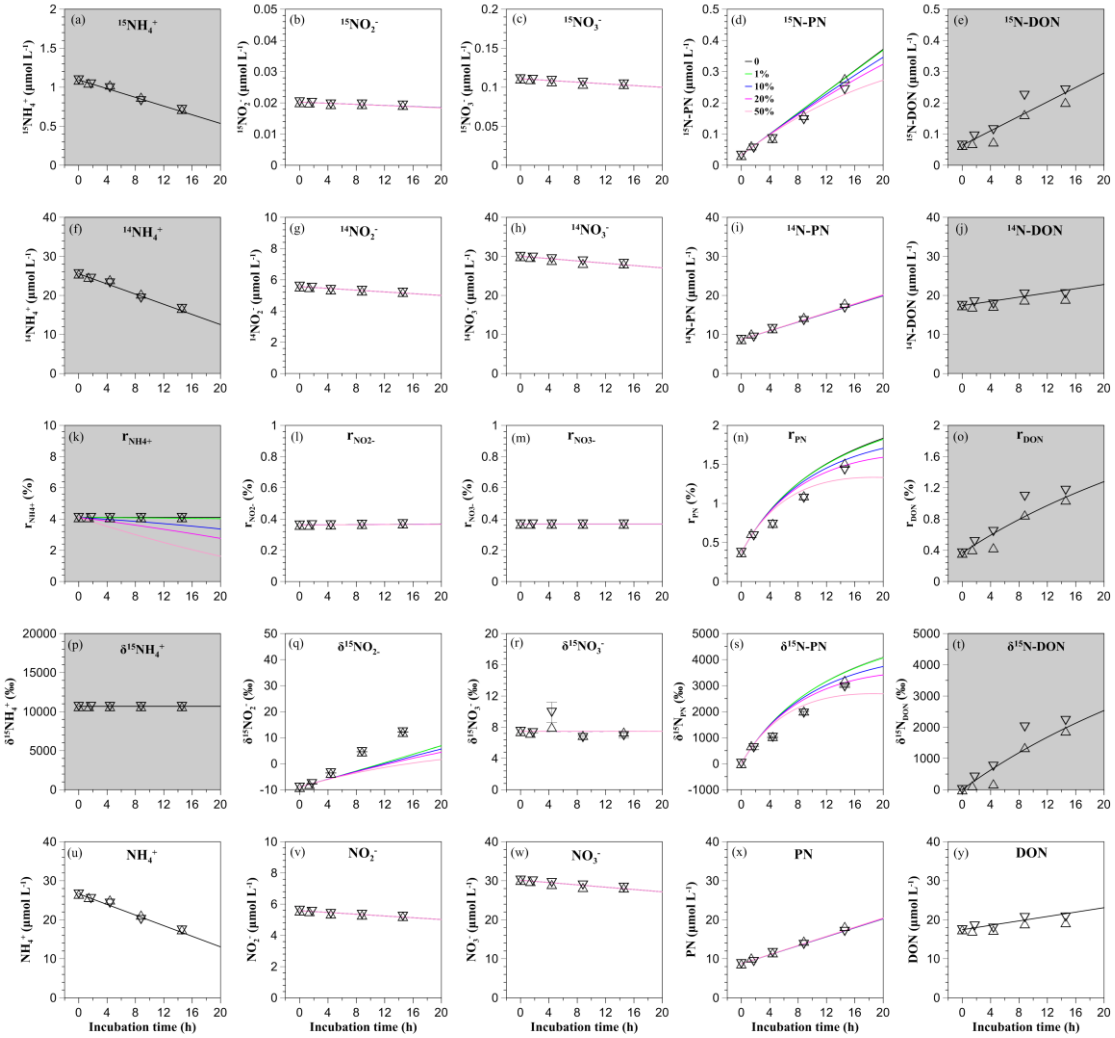
(a) $^{15}NH_4^+$
(b) $^{15}NO_2^-$
(c) $^{15}NO_3^-$
(d) ^{15}N-PN
(e) ^{15}N-DON
(f) $^{14}NH_4^+$
(g) $^{14}NO_2^-$
(h) $^{14}NO_3^-$
(i) ^{14}N-PN
(j) ^{14}N-DON
(k) r_{NH4+}
(l) r_{NO2-}
(m) r_{NO3-}
(n) r_{PN}
(o) r_{DON}
(p) $\delta^{15}NH_4^+$
(q) $\delta^{15}NO_2^-$
(r) $\delta^{15}NO_3^-$
(s) $\delta^{15}N$-PN
(t) $\delta^{15}N$-DON
(u) NH_4^+
(v) NO_2^-
(w) NO_3^-
(x) PN
(y) DON
0
1%
10%
20%
50%
Incubation time (h)

Fig. 5(B)

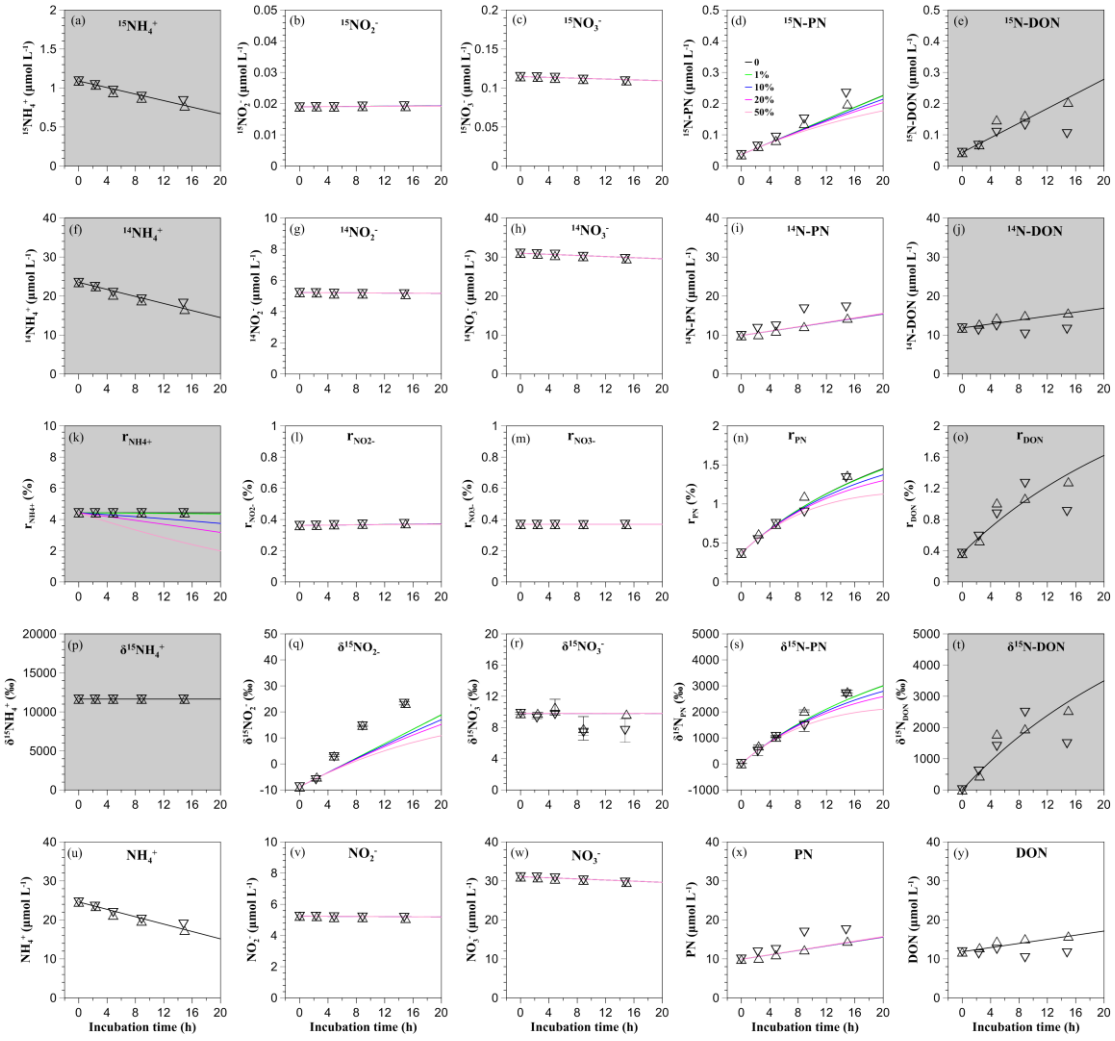
(a) $^{15}NH_4^+$
(b) $^{15}NO_2^-$
(c) $^{15}NO_3^-$
(d) ^{15}N-PN
(e) ^{15}N-DON
(f) $^{14}NH_4^+$
(g) $^{14}NO_2^-$
(h) $^{14}NO_3^-$
(i) ^{14}N-PN
(j) ^{14}N-DON
(k) r_{NH4+}
(l) r_{NO2-}
(m) r_{NO3-}
(n) r_{PN}
(o) r_{DON}
(p) $\delta^{15}NH_4^+$
(q) $\delta^{15}NO_2^-$
(r) $\delta^{15}NO_3^-$
(s) δ^{15}N-PN
(t) δ^{15}N-DON
(u) NH_4^+
(v) NO_2^-
(w) NO_3^-
(x) PN
(y) DON
0
1%
10%
20%
50%
Incubation time (h)